Chapter 4. Baseline Geochemical Survey

4-1 Outline

We implemented this series of probes with the purpose of identifying symptoms of current hydrothermal activities and traces of past hydrothermal activities as well as features of submarine sediments in the Coriolis Troughs through a geochemical method.

The general topographic structure of this survey area resembles, as described in Chapter 3, a column of troughs running from north to south, The Coriolis Troughs (in the broad sense of the word), trends NNW ~ SSE, running parallel with the survey area, but this Trough is divided by a structure trending EW into three small-scaled (narrowed) troughs (Vate Trough, Erromango Basin and Futuna Trough) running from north to south.

Bathymetric maps of the Vate Trough and the Erromango Basin had been drawn tentatively on the basis of the topographic survey performed before the survey. From these, the existence of a ridge running roughly parallel with the Erromango Basin in the neighborhood of the center of the Basin and a topographic feature forming a deep (depression) at water depths of more than 3,000m on one side (north west) of the ridge were recognized.

From these facts we concluded that the the general center of the Erromango Basin was an area with the potential existence of a spreading center, making it a most effective area for obtaining symptoms of hydrothermal activity.

We, therefore, decided to conduct probes on this Basin and planned 13 points at intervals of about 1 mile by establishing the ridge part as the center of the track lines and aligning track lines on both sides of the ridge so that the track lines transverse the Basin from east to west. Sampling points are shown in Figure 4-1-1.

Among the 13 points, samples could not be collected from 3 points. Thus, samples were only collected from 10 points (The sampling operation was repeated at the points where collection failed, so the number of sampling operations totalled 17.).

Efforts were made to collect columnar samples by employing a GC or LC at every sampling point. The length of the core tube was 4m, and deformation of the tip of the corer bit was recognized when the bit tip reached a rock mass.

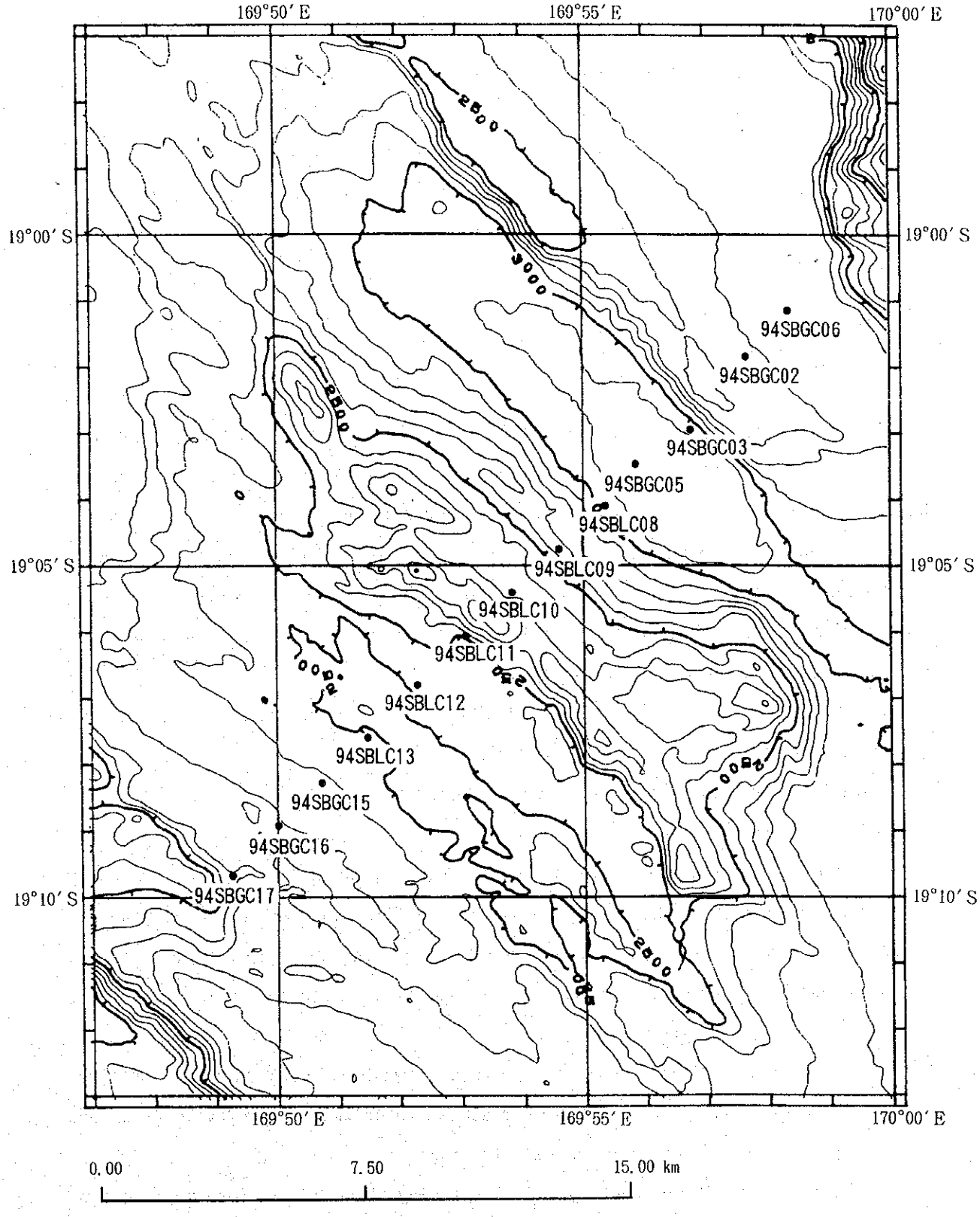

Figure 4-1-1 Location Map of Baseline Geochemical Sampling Points

In order to maintain the scales in optimum balance, we unloaded the deep-sea camera and used a subcorer when oceanographic phenomena were bad.

Data on locations, water depths, equipment used, sampling length and others related to the sampling results is shown in the Appendix Table.

Collected columnar samples were sketched, then half of the cores were sampled for chemical analysis, X-ray diffraction tests and other laboratory tests, and the remaining half were preserved.

4-2 Characteristics of Collected Samples

Collected samples were classified mainly according to their color and grain sizes. "Munsell Soil Color Charts" were used for the classification of color tones and the Wentworth Grain Size Scale (1922) was used for the classification of grain sizes.

The color tones are mainly composed of 10YR・2.5YR series (Brown series) and 5Y series (Olive series) of the "Munsell Soil Color Charts". The grain sizes are mainly composed of clay under the Wentworth (1922) grain size scale, but sand and semiconsolidated siltstone are also recognized.

The sampling results of the base-line survey classified mainly by the above-mentioned standards are shown in Figure 4-2-1 as a schematic.

Details of the sediments observed are as follows:

(1) Muddy Substances

Muddy substances are mainly composed of clay, clastic minerals, volcanic glass and calcareous shells of foraminifera. The component ratio of clay and volcanic glass is relatively high. Besides the principal components, traces of microfossils of radiolaria, diatoms and sponge spicules are recognized. Authigenic minerals are found extremely rarely.

Among principal components, a high percentage of volcanic glass is contained in these muddy substances. From this we can infer that the volcanic glass was supplied from volcanoes in and around the ridge.

It is difficult to identify details of clay through a microscope as grains are extremely fine (finer than a few μm). We presumed that the difference of color tones between the Brown series and Olive series was mainly caused by this clay as there was no other component that might cause it. Black clay was also found. We presumed it was caused by volcanic ashe.

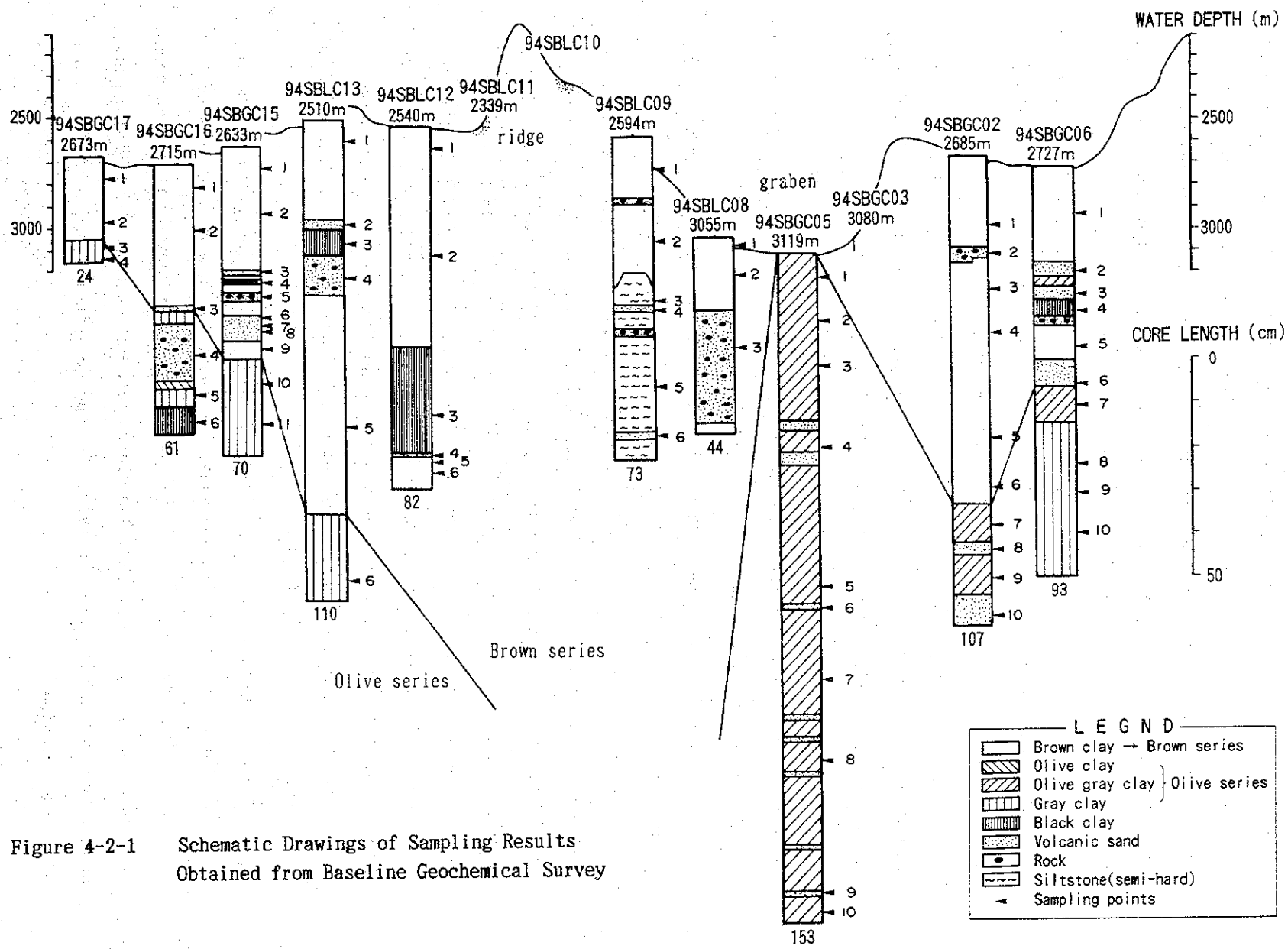

Figure 4-2-1 Schematic Drawings of Sampling Results Obtained from Baseline Geochemical Survey

Calcareous shells of foraminifera appear white. Their sizes are, on the whole, between 50μm ~ 1mm, but, when examined with a microscope, large shells are observed only as fragments. The content in muddy substances varies diversely. Most of the foraminifera fossils observed have single row arc ~ two rows spiral ~ twisted spiral chambers.

With the object of estimating the age and rate of sedimentation as well as the paleoenvironment of sediments, we conducted identification of foraminifera fossils contained in the samples collected from every point.

Among clastic minerals, plagioclase and quartz are universally observed, though in small amounts, in most of the muddy substances. Most of the plagioclase exibits acicular idiomorphic ~ hypidiomorphic characteristics and generally does not show zoning but occasional, rare zoning was observed. Quartz exibits fragmented allotriomorphic characteristics . The sizes of these clastic minerals are generally smaller than 50μm.

Some of the volcanic glass identified in the sediments of this sea area could be as fine as grains of clay. We estimate that volcanic glass exists quite universally in this area. Volcanic glass can be roughly classified into two categories, i.e. felsic glass and mafic glass. From a microscopic observation, it is presumed that the amount of felsic glass is relatively larger than that of mafic glass. This area's felsic glass exibits transparency ~ white translucency and is found as slat-shaped fragments in large quantities. Its size is generally smaller than 50μm. Felsic glass has a somewhat larger mean diameter than mafic glass. This area's mafic glass appears brown and its size is about 20μm. It exibits spheroidal ~ slat-shaped fragments with a small amount of internal foam structure.

Siliceous microfossils of radiolaria, diatoms and sponge spicules are universally observed in the survey area. The quantity, however, is very small. The radiolarias are approximately 100μm in size, and many of them have been destroyed and not well preserved. The diatoms are the Centrales in 100μm square shape, and no Pennales are observed. The sponge spicules are of wedge shape of several μm wide.

(2) Volcanic Sand (including Scoria)

The above muddy substances always comprise a few layers of sand in-between,

and the thickness of the layers ranges from less than 1 cm up to 30cm maximum. Most of the fines are around 1mm in size, while some of the scoria reach as large as 10mm. Their color is black. The boundary between the sand and the muddy substances is clear and is assumed to have accumulated over a relatively short period of time.

The major components are basaltic rock chips, volcanic glass and magnetite, while small amounts of plagioclase, quartz and pyroxene are also present. This particular sand composed mainly of pyroclastic materials are called "volcanic sand" in this chapter.

This layer produces a relatively large number of calcareous foraminiferas. This means that the volcanic activity was active at the time of accumulation and a large amount of foraminiferas died during the activity.

Samples were taken at seven points (8 samples), and the microscopic examination was conducted with thin section so as to specify detailed rock classification and mineral composition of the components.

(3) Semi-Concrete Siltstone

The sampling conducted on the NE slope of the central ridge has brought semi-concrete siltstone. In terms of grain size, it may belong to clay, but in this chapter we have defined it as silt rock.

While its color tone shows 2.5YR series (Brown series), the macroscopic test shows more Gray series than the 2.5YR (Brown) series clay on a higher layer.

Compared with the afore-mentioned muddy substances, the main components of the semi-concrete silt rock do not differ much although the ratio of diatoms is slightly higher.

It is clear, however, that it shows an inconsistent relation with the clay on a higher layer.

In order to determine the accumulation age and the ancient environment, we have conducted microfossil examination.

The most conspicuous aspect in the vertical continuum seen in the sediments in this area is their color tone. In other words, the general rulethat radiolaria, i.e. 10YR · 2.5YR series (Brown series), will distribute relatively on a higher layer than 5Y series (Olive series) sediments is proved valid at every point. The boundary

between the two series is irregular;sometimes they are clearly divided by volcanic sand but sometimes they show a transitional relation. There is no clear difference between the two series as to the quantitative ratio of their components. We can presume that these facts indicate that the former exibits in an oxidized environment and the latter in a reduction environment.

But we need more information about clay minerals and chemical composition to make a definite conclusion.

The depth of boundary between Brown series sediments and Olive series sediments (the base depth of 10YR ～ 2.5YR series sediments) trends to become deeper as we approach the ridge in the central part of the track line. This indicates that the oxidized environment becomes stronger in the ridge. This tendency is particularly prominent in the southwest part of the track line.

The area where the reduction environment appears closest to the sea-floor is the deepest part of the Basin located in the northeastern part of the base-line track line.

Furthermore, distribution of semiconsolidated siltstone that exibits inconsistent relations with its upper layers is identified at the portion deeper than 30cm from the sea-floor by the sampling conducted on the northeastern slope of the ridge.

From these facts we know that the oxidized environment reached to deep areas, that old sediments were distributed right beneath the oxidized environment and that the possibility of being affected by some kind of tectonic movement was high. We could not identify any sign of hydrothermal deposits by this survey.

<Microfossil identification of muddy substances>

With the objective of estimating the age of sediments and rate of sedimentation as well as their paleoenviroment, we conducted an identification of foraminifera fossils contained in the muddy substances collected.

The identification was conducted comprehensively not only on the samples collected through the baseline geochemical survey but also on the samples collected through the ore deposit investigation.

A total of 31 samples were vertically collected from 10 baseline points and 13 samples were collected through the ore deposit investigation.

Samples for appraisal were washed with water on a 200-mesh (74μm) screen, then dried with a thermostatic dryer. Hard samples that could not be broken by this method

were processed by a naphtha method. The naphtha process is as follows:first, crushed raw ores are placed in a thermostatic dryer and heated at about 100℃. Then, the samples are soaked in naphtha for 1 ～ 2 hours. After they are fully permeated, they are rinsed in hot water, and boiled to evaporate the naphtha, followed by screening with a 250-mesh (63μ) sieve, washing with water thoroughly and drying with a thermostatic dryer. When a rock did not fully break down by one process, this method was repeated two or three times.

Dried samples were divided by a divider so as to create 200 ～ 300 individual samples. These individuals became the samples for microfossils studies. As for the appraisal of planktonic foraminifera, only individuals larger than 80 mesh (150μ) were selected for community analysis. The appraisal of species and counting of numbers of divided individuals was conducted under a microscope. The existence of fossils other than foraminifera and the existence of volcanic clastics were also recorded during the microscopic examination.

The results of the appraisal showed that the greater part of the samples are planktonic foraminifera with low levels of benthic foraminifera.

Photographs of typical species of planktonic foraminifera are shown in Figure 4-2-2, the detected results of planktonic foraminifera are shown in Table 4-2-1 and the detected results of benthic foraminifera are shown in Table 4-2-2.

(Planktonic foraminifera)

The fossil communities of planktonic foraminifera contained in these sediments ubiquitously include *Globigerinoides ruber, Globigerinoides sacculifer, Globigerinoides conglobatus, Orbulina universa, Pulleniatina obliquiloculata, Neogloboquadrina dutertrei, Globigerinita glutinata, Hastigerina pelagica, Globorotalia crassaformis crassaformis, Globorotalia cultrata cultrata, Globorotalia tumida tumida, Globorotalia truncatulinoides* and *Globigerinella aequilateralis. Bolliella calida calida* and *Bolliella calida praecalida* are also ubiquitously observed, though the incidence of occurrence is low.

On the other hand, the samples show very low levels of the *Globigerina* genus. From the facts that (1) every *Pulleniatina* genus is dextrally spiraled and that (2) *Globorotalia tosaensis* does not appear except from the lower part of the same samples, we can determine that this community corresponds to the zone between the upper part of N22 and N23 under the fossil zone classification of low-

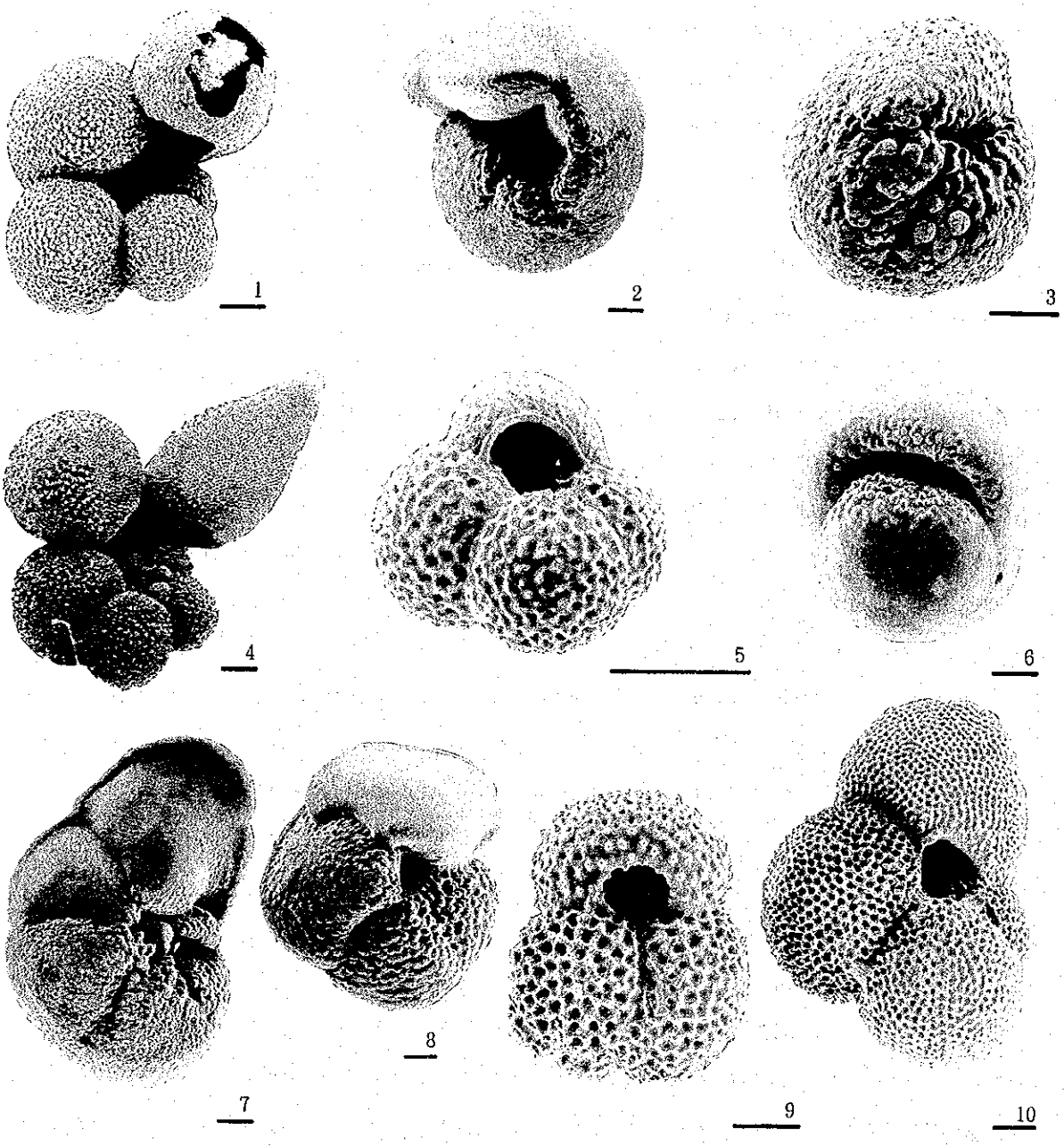

Scale bars: 100 μ m

1. *Bolliella calida calida* (Parler). Umbilical view, Sample from 94SBGC02, 10-20cm.
2. *Globorotalia truncatulinoides* (d'Orbigny). Umbilical view, Sample from 94SBGC02, 91-100 cm.
3. *Globorotalia tosaensis* Takayanagi and Saito. Umbilical view, Sample from 94SBLC09, 45-67 cm.
4. *Bolliella adamsi* Bannaer and Blow. Umbilical view, Sample from 94SBLC13, 100-110 cm.
5. *Globigerina rubescens rubescens* Hofker. Umbilical view, Sample from 94SBLC13, 100-110 cm.
6. *Pulleniatina finalis* Banner and Blow. Umbilical view, Sample from 94SDLC09, 10-20 cm.
7. *Globorotalia tumida flexuosa* (Koch). Umbilical view, Sample from 94SDLC09, 136-146 cm.
8. *Globorotalia crassaformis crassaformis* (Galloway and Wissler). Umbilical view, Sample from 94SBLC12, 0-10 cm.
9. *Globigerinoides ruber* (d'Orbigny). Umbilical view, Sample from 94SBLC12, 0-10 cm.
10. *Globigerinoides sacculifer* (Brady). Umbilical view, Sample from 94SBLC02, 0-10 cm.

Figure 4-2-2 Species of the Typical Foraminifera Fossils (Planktonic Foraminifera)

Table 4-2-1 List of planktonic forraminiferal fossils in the stusied cores

Sample	Depth	Abundance	Preservation	Bolliella adamsi Bannerand Blow	Bolliella calida calida (Parker)	Bolliella calida praecalida (Blow)	Bolliella praeadamsi Chaproniere	Candeina nitida d'Orbigny	Globigerina (Beella) digitata digitata (Brady)	Globigerina (Beella) digitata praedigitata Parker	Globigerina (Globigerina) bulloides bulloides d'Orbigny	Globigerina (Globigerina) falconensis Blow	Globigerina (Globoturborotalia) decoraperta Takayanagi and Saito	Globigerina (Globoturborotalia) rubescens rubescens Hofker	Globigerina (Globoturborotalia) rubescens rubescens Hofker (pink)	Globigerinella aequilateralis (Brady)	Globigerinita glutinata Egger	Globigerinoides conglobatus Brady	Globigerinoides elongatus d'Orbigny	Globigerinoides immaturus LeRoy	Globigerinoides pyramidalis (Van den Broeck)	Globigerinoides ruber (d'Orbigny)	Globigerinoides sacculifer (Brady)
94SBGC06	10-19.	F	M		3	1		3							X	25	9	28	16	66	3	67	31
	72-75	F	M		13	18			1		4				X	31	73	6	8	17		63	3
94SBGC02	10-20.	A	G		2		8	3	2					2	X	22	21	20	20	63	4	121	28
	35-45	A	G	X			X	3								31		36	5	38	6	30	31
	70-79	A	G		4	4			1		3			1	X	22	18	23	12	25	3	47	18
	91-100	A	G		12	6		1		1	7			1		18	28	15	8	32	1	127	22
94SBGC05	10-20.	R	M		5	7		9		5	1					25	36	30	18	60	6	68	35
	70-80	R	M		2	7		4	2		1					15	29	37	45	87	5	77	26
	100-110	R	M		1	1		3			1					15	9	30	9	61	5	45	31
94SBLC08	4-14	C	G		3	2		5								22	2	51	6	75		50	35
	20-30	R	G		1											18		89	1	54	4	13	35
94SBLC09	0-13	A	G		10	1		2	1						X	52	20	27	15	46	2	73	18
	18-28	A	G		13	1				3	5	3	1	1	X	22	42	6	22	27	1	118	13
	45-67	R	M			4		1								25	12	31	32	53	3	87	28
94SBLC12	0-10	A	G		1						1					26		31	16	56	1	35	35
	25-35	A	G	X	2	1		1	1	1				1	X	20	20	11	26	59		99	19
	62-72	C	G		6	2		1	2		1					28	10	17	6	20	1	48	9
	75-82	C	G		4	7				1	6			2		14	26	12	12	20	3	79	14
94SBLC13	0-10	A	G		6			1							X	14	13	31	19	52		53	22
	31-40	C	G		1										X	13		34	10	85		62	52
	43-50	C	G						2		1				X	32	11	22	9	48		71	16
	65-75	C	G		5	2	2	2	1		3	1			X	38	5	6	33	47	1	75	26
	100-110	C	G	X	7		1		2			1			X	19	16	16	19	20		72	15
94SBGC15	10-20.	A	G			2		1						2	X	8	12	21	23	31		111	14
	38-41	R	M													16	7	33	14	53		37	20
	44-48	C	G		X	4			3						X	16	5	33	11	37		75	13
	57-70	R	M		3	2			1				1	1	X	18	13	17	21	49	1	75	20
94SBGC16	10-19.	A	G		X	1		2							X	38		43	8	57	3	18	58
	36-49	R	G					1								19	11	12	22	78	1	103	16
	49-55	F	M			4	1	2						1	X	16	10	13	12	47		77	15
94SBGC17	11-19.	C	G		X	2		3						1	X	19	3	32	15	34	1	37	25
94SDLC09	10-20.	A	G					2	1	1					X	50	2	45	7	37	5	16	25
	49-57	A	G		3	2			1		1				X	23	5	32	16	26	2	45	15
	91-110	A	G		3	1					1			1	X	16	7	32	13	22	3	67	9
	136-146	A	G		1	9				1	8	1		3		23	65	18	9	18		109	14
94SDLC13	25-30	A	G		9		2		1						X	16	17	27	11	32		80	8
	60-70	R	M											1		4	2	10	3	24	3	17	14
94SDLC12	10-20.	R	M		2	1		1			1	2		1		11	2	27	10	34	1	60	32
	35-45	F	M		1	1					2					19	4	34	24	69	1	120	42
	60-70	R	M		1	2										1	3	3	2	13	1	17	2
94SDLC15	10-17.	R	M	1	2	2							1			22	10	9	15	67		78	18
	22-30	C	G		4						1				X	21	1	21	41	55	1	61	23
	52-62	R	M		4	2						1		1		10	9	4		17	1	57	7
	62-69	C	G		3	2				1	1		1			11	6	15	12	20	1	63	19

Sample	Depth	Globigerinoides tenellus Parker	Globorotalia (Globoconella) inflata (d'Orbigny)	Globorotalia (Globorotalia) cultrata cultrata (d'Orbigny)	Globorotalia (Globorotalia) cultrata neoflexuosa Srinivasan, Kennett, and Be	Globorotalia (Globorotalia) tumida flexuosa (Koch)	Globorotalia (Globorotalia) tumida tumida (Brady)	Globortalia (Globorotalia) ungulata Bermudez	Globorotalia (Obandyella) bermudezi Rogl and Bolli	Globorotalia (Obandyella) scitula scitula (Brady)	Globorotalia (Truncorotalia) crassaformis crassaformis (Galloway and Wissler)	Globorotalia (Truncorotalia) crassaformis ronda Blow	Globorotalia (Truncorotalia) crassaformis viola (Blow)	Globorotalia (Truncorotalia) crassula Cushman and Stewart	Globorotalia (Truncorotalia) tosaensis Takayanagi and Saito	Globorotalia (Truncorotalia) truncatulinoides (d'Orbigny)	Hastigerina pelagica (d'Orbigny)	Hastigerina praesiphonifera Blow	Neogloboquadrina dutertrei (d'Orbigny)	Neogloboquadrina humerosa (Ehrenberg)	Neogloboquadrina spp.	Orbulina universa d'Orbigny	Orbulina bilobata d'Orbigny	Pulleniatina finalis Banner and Blow	Pulleniatina obliquiloculata (Parker and Jones)	Pulleniatina primalis Banner and Blow	Sphaeroidinella dehiscens dehiscens (Parker and Jones)	Tenuitella clemenciae (Bermudez)	"Tinophodella" evoluta Fordham		Total
94SBGC06	10-19.		1	1			1				2		3			3	7		2			21		X	1		1	1			296
	72-75						1	1		1							2		3			9		X	1				1		256
94SBGC02	10-20.			1						1			1						4			14		X							337
	35-45									1	3						4		3			35			3		3				232
	70-79				2					2	3					1	4		10			8			4	1					216
	91-100	1	4	1	1		2			3	6			2		6			12	1		16		X	5	3					342
94SBGC05	10-20.			1			1			2			2			1			1			16									329
	70-80	1		1					1	1	4		3			2	1		3			13			1		2				370
	100-110									2	5					1			3			25									247
94SBLC08	4-14			1						2	5	1	8			1			10			24		X	1	1	2				307
	20-30		1	7			1	1			11	1	3	1		2			8			17			3	1	10				282
94SBLC09	0-13			3	3		1				1	1	1			3	3	2	9			36		X	4						334
	18-28	2	1	20							3	3	1	1					15	1		7		X	1	5					338
	45-67	1	3	1	2							3	2		1		1	1	16			4			4						315
94SBLC12	0-10	1									2		1			2	1		6			32		X	1		1				249
	25-35	1															2		2			12			1	3	1		1		283
	62-72		1	1			X			2	1		2	1		2	2		4	1		16			2	4					190
	75-82		5	9		2	1	2		3	4		1			1			14	4		14		X		4					264
94SBLC13	0-10			2						2	2		1			1	1		3			23		X							246
	31-40						1	1		1			4				1		3			44			4						316
	43-50																2	1			1	16									232
	65-75						1						1					2	8			17	1		5	1					283
	100-110	2		3					X	1	4		1	1		4	2	1	8			17			2	2					236
94SBGC15	10-20.																					22		X			1				248
	38-41			1		2				1	1		4						1			8			2		1				201
	44-48												3			X			4			23					3				230
	57-70	1					1			1	5								7	1		4				1					243
94SBGC16	10-19.	1									1					1			9			24		X	1		1				266
	36-49	1									1	1	4						2	1		1			1	3					278
	49-55			1							6		1				2	1	3			20		X	3						235
94SBGC17	11-19.			2			1				5		1	1		2	3	1	5			51			4		1				249
94SDLC09	10-20.		1				1				4		1				2		1	1		51		X							253
	49-57			X						X	4		1				1		9	1		15		X	9	7					218
	91-110		9	5	2		1				11	2	3				1	2	17	5		14		X	2	1					250
	136-146			11	1	1	5		1	4	9	5							19			9			6	4					354
94SDLC13	25-30	1		1			X		1		1		1			X			2	3		29		X	6	1	1				250
	60-70						1	3					2						2						1						87
94SDLC12	10-20.			1							6		4						17		1	9			9	1	1				234
	35-45			1	3		1			1	7	1	4					1	14	1		5			18	3					377
	60-70		1	4			2				3	1	1			1			6						1	5					70
94SDLC15	10-17.			1		1					3						1	1	2			3		X		2					239
	22-30		4		6	1				2	8	2	2			1			23			10			6	10					304
	52-62		2	8	1		1			1	5	1							6			1			6	1					146
	62-69		3	17	2	1	3			4	9	7	2		1	2			26			7			4	3					246

Table 4-2-2 List of benthic foraminiferal fossils in the studied cores

	SBGC06 10-19	SBGC06 72-75	SBGC02 10-20	SBGC02 35-45	SBGC02 70-79	SBGC02 90-100	SBGC05 10-20	SBGC05 70-80	SBGC05 100-110	SBLC09 18-28	SBLC12 25-35	SBLC12 62-72	SBLC12 75-82	SBLC13 0-10	SBLC13 31-40	SBLC13 43-50	SBLC13 65-75	SBLC13 100-110	SBGC15 10-20	SBGC15 38-44	SBGC15 44-48	SBGC15 57-70	SBGC16 10-19	SBGC16 36-49	SBGC16 49-55	SBGC17 11-19	SBLC08 20-30	SDLC09 49-57	SDLC09 91-101	SDLC12 10-20	SDLC12 35-45	SDLC12 60-70	SDLC09 136-146	SDLC13 25-30	SDLC15 62-69	SDLC15 22-30
AGGLUTINATED FORAMINIFERA																																			
Bathysiphon sp. A														1																					
B. spp.														7																					
Cyclammina cf. cancellata				1																															
Eggerella bradyi		1																									1	1							
E. pacifica											1																								
E. ? sp.			1																																
Haplophragmoides sp.														1																					
Jaculella ? sp.														1																					
Karreriella cf. chapapotensis														2		1																			
Miliammina sp.																												1							
Pelosina ? sp.													1																						
Rhabdammina sp.														1																					
Rhizammina ? sp.	1																																		
Trochammina ? sp.		1		1																		1											1		
Gen. et sp. indet.											2						1								1										
CALCAREOUS FORAMINIFERA																																			
Amphicoryna scalaris sagamiensis																									1										
Angulogerina sp.		1																																	
Astacolus sp.		1																									1								
A. ? sp.																		1																	
Astrononion sp.	1																																		
Bolivina albarossi															1																				
B. ? albarossi																								2											
B cf. incrassata																								1											
B. compacta																	1																		
Bolivinita quadrilatera																1	1	1																	
Bolivinoides ? sp.		1																																	
Brizarina ? sp.																											1								
Chilostmella oolina													1												1										
Cibicides refulgens																											1								
C. subdepressus														1																					
C. cf. subdepressus																											1								
C. spp.																								2											
Cibicidoides basilanensis																																	1		
Dentalinoides ? sp.															1									1			1	2							
Elphidium cf. reticulosum																						1													
Fissurina marginata																																		1	
F. sp.		1																																	
F. ? sp.																								1											
Globocassidulina gemma																						1													
G. moluccensis																																		1	1
G. subglobosa							1											1	1					1				2		1					
Grabratella ? sp.																													1						
Gyroidina girardana							1															1					1						1		
Hanzawaia bubnanensis																																		1	
Hoeglundina elegans	1																																		1
Hyalinea ? sp.																								2											
Lagena sulcata spicata																												1							
Laticarinina pauperata																			1																
Lenticulina sp.																													1						
Melonis pacificus																											2								
M. pompiloides									1																								1		
M. sp.																								1											
Oolina scalariformis					1																														
Oridorsalis umbonatus									2																				1						
O. sp.	1																																		
Parafissurina curta																																	1		
P. subcircularis		1																																	
Pullenia bulloides					3	1	1	2							1							1								1					
P. quinqueloba																															1				
Pyrgo dapsilis																			1																
P. depressa							1																										2		
P. ecuadorensis		1																																	
P. murrhina				1		2				1		1	1												1									1	
P. cf. perviana						1																													
P. sp.																													1						
Pyrulinoides sp.																												1							
Quinqueloculina acuticarinata																													1						
Q. seminulum														1																					
Q. vulgaris							1																												
Q. cf. vulgaris																			1																
Q. sp.		1																															1		
Rosalina sp.								1																			1								
Triloculina cf. brevidentata														1																					
T. trigonula																				1															
Uvigerina peregrina																						1													
U. proboscidea	1																		1																
U. sp.										1																									
Valvulineria sp.																1																			
Gen. et. sp. indet							3																	2	2										
TOTAL	5	8	1	3	5	8	5	5	1	3	1	2	3	15	4	2	3	6	1	1	1	4	1	13	5	1	9	5	8	1	1	2	6	3	2	2

latitude regions established by Blow (1969).

Accordingly, we can infer that the geological ages of most of these sediments is later than the Middle Pleistocene Epoch. Chaproniere (1991) proposes a classification of fossil zones by subdividing Blow's (1969) N22 and N23 zones into 7 subzones. As this survey area calls for discussing the geological age of the Pleistocene in detail, we used the subzones of Chaproniere (1991) for determining the geological age (Fig. 4-2-3). The index datum of each species used for defining fossil zones and the geological age of the index datum were based on the geochronologic classification of Berggren et al. (1985). As these index datums are related to the low-latitude communities, they can be applied to this survey area without retouching. *Globigerinoides ruber* (pink), however, did not occur in the samples analyzed. So, it is questionable to use *Globigerinoides ruber* (pink) as an index datum.

he following index datums was used for this year's survey:

1) the appearance of *Bolliella adamsi*
2) the disappearance of *Globorotalia tumida flexuosa*
3) the appearance of *Bolliella calida calida*
4) the appearance of *Pulleniatina finalis* and *Bolliella praeadamsi*
5) the disappearance of *Globorotalia tosaensis*

The consolidation of 94SDLC12, 13 and 15, among the samples analyzed, was relatively advanced. So the sediments collected from these points could not be processed by the naphtha method. Most of the other sediments were soft and could be processed by washing with water only. Diatoms, foraminifera, radiolaria, coccids, shell fragments and echinoid spines were contained in the sediments, but the occurrence of foraminiferan and radiolarian fossils was overwhelmingly abundant. As for foraminifera, planktonic foraminifera accounts for a majority and benthic foraminifera occurs seldom. The sediments generally contain pyroclastic materials, especially the sediments from 94SBGC06 to 94SBGC17 frequently contain silt-sized to pebble-sized particles of pyroclastic materials. On the other hand, there is a tendency for pyroclastic materials to decrease at 94SDLC12 ~ 94SDLC15. Figure 4-2-4 sums up the distribution of stratigraphic fossil zones in each core obtained by this year's survey.

The state of preservation and estimated age of planktonic foraminifera at each sampling point are discussed hereunder.

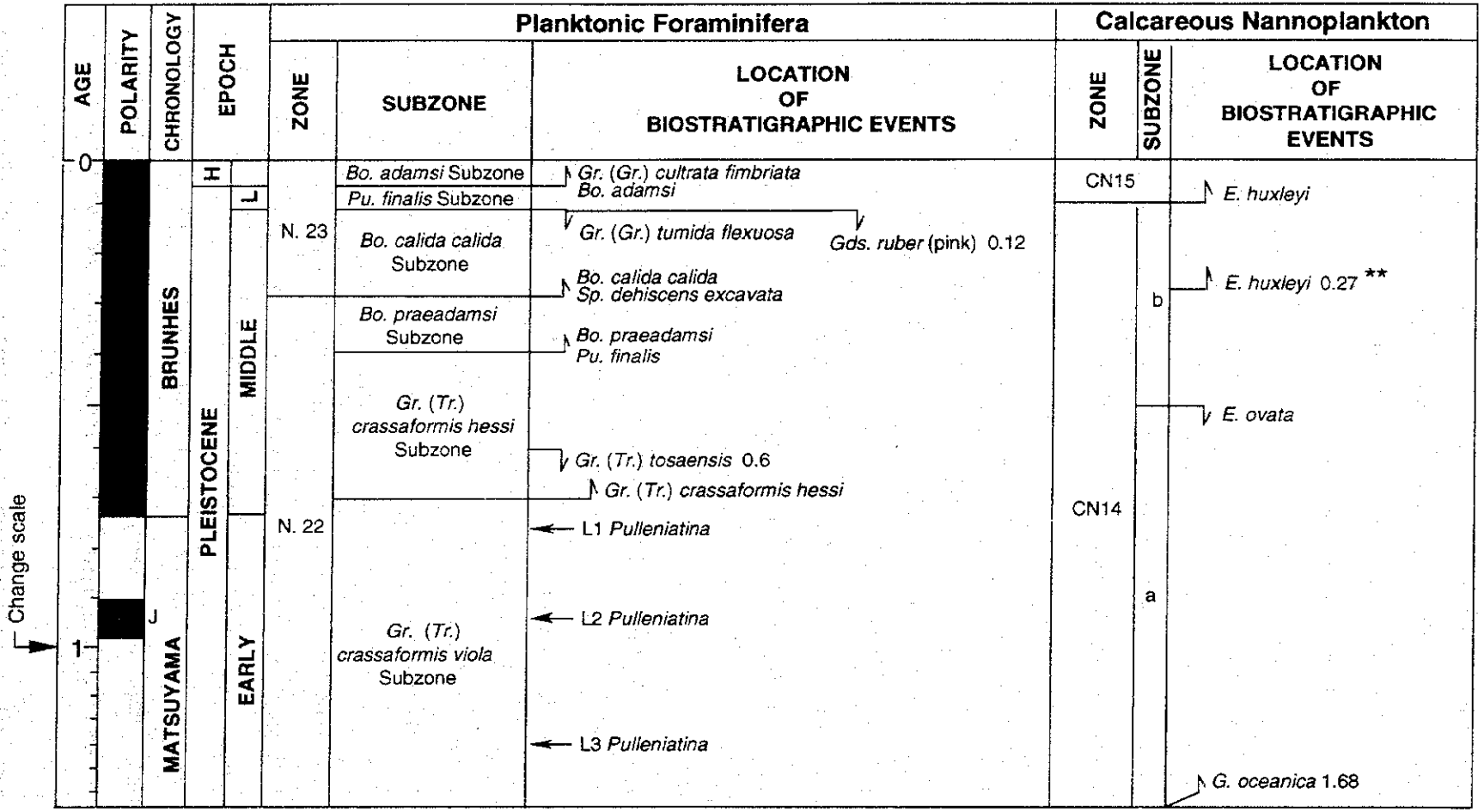

Calcareous nannoplankton
E. : *Emiliania*
G. : *Gephyrocapsa*

Planktonic Foraminifera
Bo. : *Bolliella*
Gds. : *Globigerinoides*
Gr. (Gr.) : *Globorotalia*
Gr. (Tr.) : *Truncorotalia*
Pu. : *Pulleniatina*

Figure 4-2-3 Biostratigraphic zonal scheme and events in the low latitude regions (Person et al., 1991 : Chaproniere, 1991)

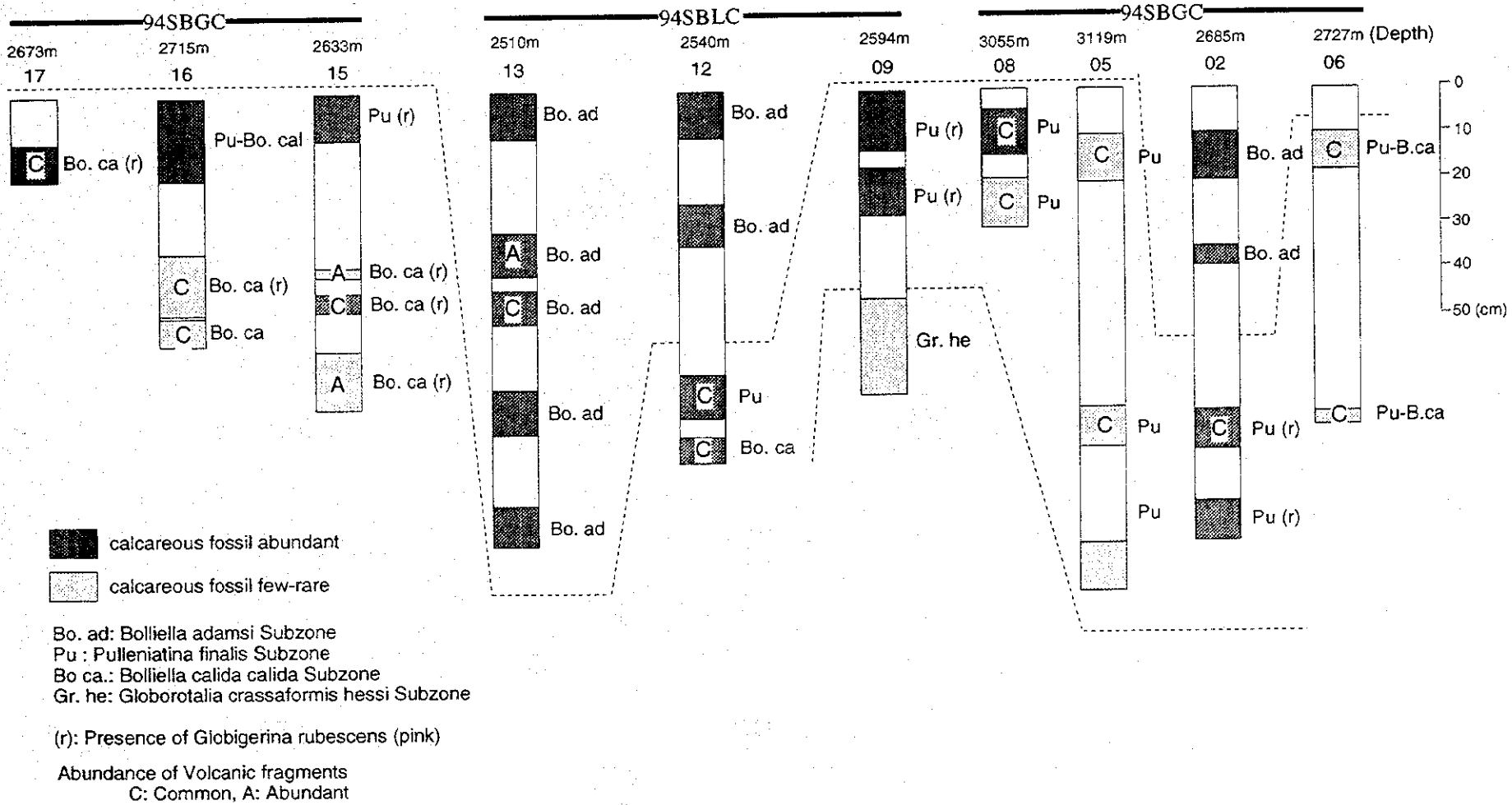

Figure 4-2-4 Stratigraphical distribution of planktonic foraminiferal zones in the studied cores (1)

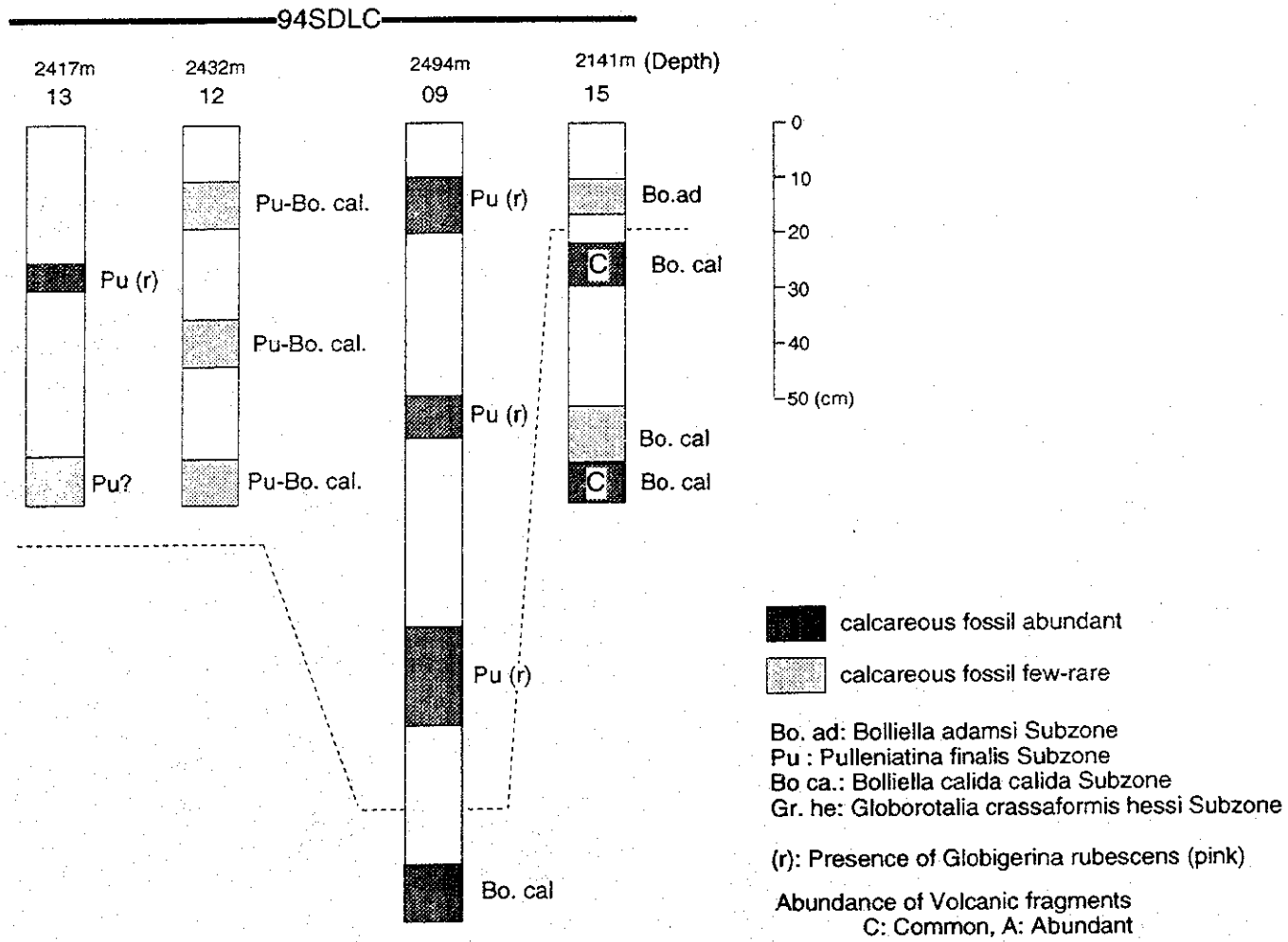

Figure 4-2-4 Stratigraphical distribution of planktonic foraminiferal zones in the studied cores (2)

- 94SBGC06 (water depth: 2,727m)

Sediments are composed of silt containing pyroclastic materials and not abundant in calcareous fossils.

Bolliella calida calida, Pulleniatina finalis and pink individuals of *Globigerina rubescens rubescens* (hereinafter referred to as *G. rubescens* (pink)) are identified in the community of planktonic foraminifera which indicates that it corresponds to the subzone of *Pu. finalis-* ~ *Bo. calida calida.*

- 94SBGC02 (water depth: 2,685m)

Sediments are calcareous and rich in planktonic foraminifera. Although volcanic particles are few, pebble-sized pyroclastic particles become abundant in the 70-79cm horizons which indicates the resumption of volcanic activities. As *Bolliella adamsi* occurs at 45cm depth from the surface layer, the layers above this level correlate with the *Bo. adamsi* subzone. Lower layers include *Pu. finalis, B. calida calida* and *G. rubescens* (pink) so it is inferred that they correspond to the Pu. finalis subzone.

- 94SBGC05 (water depth: 3,119m)

The sediments consisting of volcanic silt and sand, but lacking in fossils, are overwhelmingly rich in sand-sized volcanic particles but pebble-sized particles are also observed at the lowest depth (100cm). However, contained fossils are well preserved and large-sized individuals are also observed.

There is high possibility that these fossil communities are turbidite sediments carried in from shallow sea regions together with pyroclastic particles.

Bo. calida calida ubiquitously occur in the sample of this core, but *Pu. finalis* and *G. rubescens* (pink) don't. As *Gr. tumida flexuosa* does not occur in this sample, it is inferred that this sample corresponds to the *Pu. finalis subzone.*

- 94SBGC08 (water depth: 3,055m)

This core is rich in volcanic sand and pebble particles. The upper part (up to 14cm) is rich in fossils and the lower part (20-30cm) is less abundant but fossils in both parts are well preserved. Its fossil community contains *Bo. calida calida* and *Pu. finalis* so it correlates with the *Pu. finalis*

subzone but *G. rubescens* (pink) does not occur in this sample.

- 94SBGC09 (water depth: 2,594m)

The sediments are calcareous and rich in planktonic foraminifera. There are few volcanic particles in the core.

Bo. calida calida, *G. rubescens* (pink) and *Pu. finalis* occur in the part from the surface layer to the 28cm level, so it is presumed that this part correlates with the *Pu. finalis* subzone. *Gr. tosaensis*, however, occurs in the lowest part (45-67cm) which indicates the possibility of corresponding to the *Gr. crassaformis hessi* zone.

- 94SBGC12 (water depth: 2,540m)

The sediments are calcareous and rich in planktonic foraminifera and radiolaria fossils. *Bo. adamsi* occurs from 25-35cm deep, so the upper levels from this level correspond to the *Bo. adamsi* subzone. *Gr. tumida flexuosa* occurs from the lowest part (75-82cm), so the lower parts under this level correlate with the *Bo. calida calida* subzone.

- 94SBGC13 (water depth: 2,510m)

Most of the sediments in the surface layer (up to 10cm) are calcareous but two horizons (31-41cm and 43-50cm) are rich in pyroclastic materials. The former horizon contains many pebbles of about 5mm size. The portion lower than the 50cm-horizon transit again to calcareous sediments. The entire core is rich in fossils and they are well preserved. As *Bo. adamsi* occurs in the lowest part(100-110cm), the entire core correlates with the *Bo. adamsi* subzone. *G. rubescens* (pink) occurs throughout the core.

- 94SBGC15 (water depth: 2,633m)

The surface layer (10-20cm) and the 44-48cm horizon are composed of calcareous sediments and rich in planktonic foraminifera. But the 38-41cm and 57-70cm horizons are rich in pyroclastic materials and fossils rarely occur in these two horizons. Especially, the 38-41cm horizon is rich in pebble-sized volcanic particles. *Gr. tumida flexuosa* occurs from the 38-41cm horizon and the levels lower than this horizon correlate with the *Bo. calida calida* subzone. *Pu. finalis*

and *G. rubescens* (pink) occurs in the surface layer (0-10cm), which can be correlated with the *Pu. finalis* subzone.

- 94SBGC16 (water depth: 2,715m)

The surface layer (10-19cm) is calcareous sediments and rich in planktonic foraminifera. The parts below this layer become rich in pyroclastic materials and poor in fossils. Especially, small pebbles consist of pyroclastic materials increase in the 36-49cm horizon. *Bo. calida calida, G. rubescens* (pink) and *Pu. finalis* occur in the surface layer which infers that the surface layer correlates with the *Pu. finalis* subzone. *Bo. calida calida* does not occur in the layers below the surface layer. We infer that the lower layers have been affected by the action of solution. Fossils in these two horizons (36-49cm and 49-55cm) are not so well preserved and the number of individuals decreases extremely.

This core can be relatively clearly correlated with 94SBLC15 from the lithofacies, so it is inferred that it correlates with the *Bo. calida calida* though *G. calida calida* does not occur in the lower part.

- 94SBLC17 (water depth: 2,673m)

The sediments are silt containing abundant pyroclastic materials. Well preserved fossils occur in these sediments considerably. Because *Bo. calida calida* and *G. rubescens* (pink) occur in the sediments, it is inferred that the core correlates with the *Pu. finalis* subzone. One individual of *Gr. tosaensis* occurs in the core, but it is considered to be a result of resedimentation.

- 94SDLC09 (water depth: 2,494m)

Whole sediments are calcareous and volcanic particles are very few. Also rich in fossils. *Gr. tumida flexuosa* occurs fromthe lowest part (1130-146 cm), with lower levels correlating with the *Bo. calida calida* subzone and higher levels higher correlating with the *Pu. finalis* subzone. This core is also abundant in *Bo. calida calida, G. rubescens* (pink) and *Pu. finalis.*

- 94SDLC12 (water depth: 2,432m)

The sediments are composed of considerable amount of consolidated lutaceous rocks and are poor in fossils.

Especially, the surface layer is rich in small individuals which are poorly preserved, so it is inferred that the surface layer has been affected by the action of solution. Also poor in volcanic particles. Among the index species indicating geological ages, only*Bo. calida calida* occurs in this core, so detailed ages are uncertain.

In all likelihood, it may correlate with the *Pu. finalis* ~ *Bo. calida calida* subzone.

- 94SDLC13 (water depth: 2,417m)

The upper part (25-30cm) of the sediments is calcareous and abundant in fossils but the lower horizon (60-70cm) is, like 94SDLC12, hard and consolidated. Both horizons are poor in pyroclastic materials. From the fact that *Bo. calida calida, G. rubescens* (pink) and *Pu. finalis* occur in the upper part, it correlates with the *Pu. finalis* subzone. The lower part is very poor in fossils and the community is presumed to be affected by the action of solution. Therefore, detailed geological ages are uncertain.

- 94SDLC15 (water depth: 2,673m)

Whole sediments are solidified. The samples of this core can be divided into lutaceous rocks rarely containing fossils (the 10-17cm horizon and the 52-62cm horizon) and lutaceous rocks containing calcareous fossils (the 22-30cm horizon and the 62-69cm horizon). The former rarely contains pyroclastic particles but, in the sediments of the latter, the 22-30cm horizon is considerably rich in sand or pebble-sized particles and the 62-69cm horizon contains them off and on. The samples in the highest part contain *Bo. adamsi*. Levels above it correlate with the *Bo. adamsi* subzone and lower levels correlate with the *Bo. calida calida* subzone.

Following is a description of the community composition of planktonic foraminifera. Component ratios classified bygenus of each sample are shown in Figure 4-2-5.

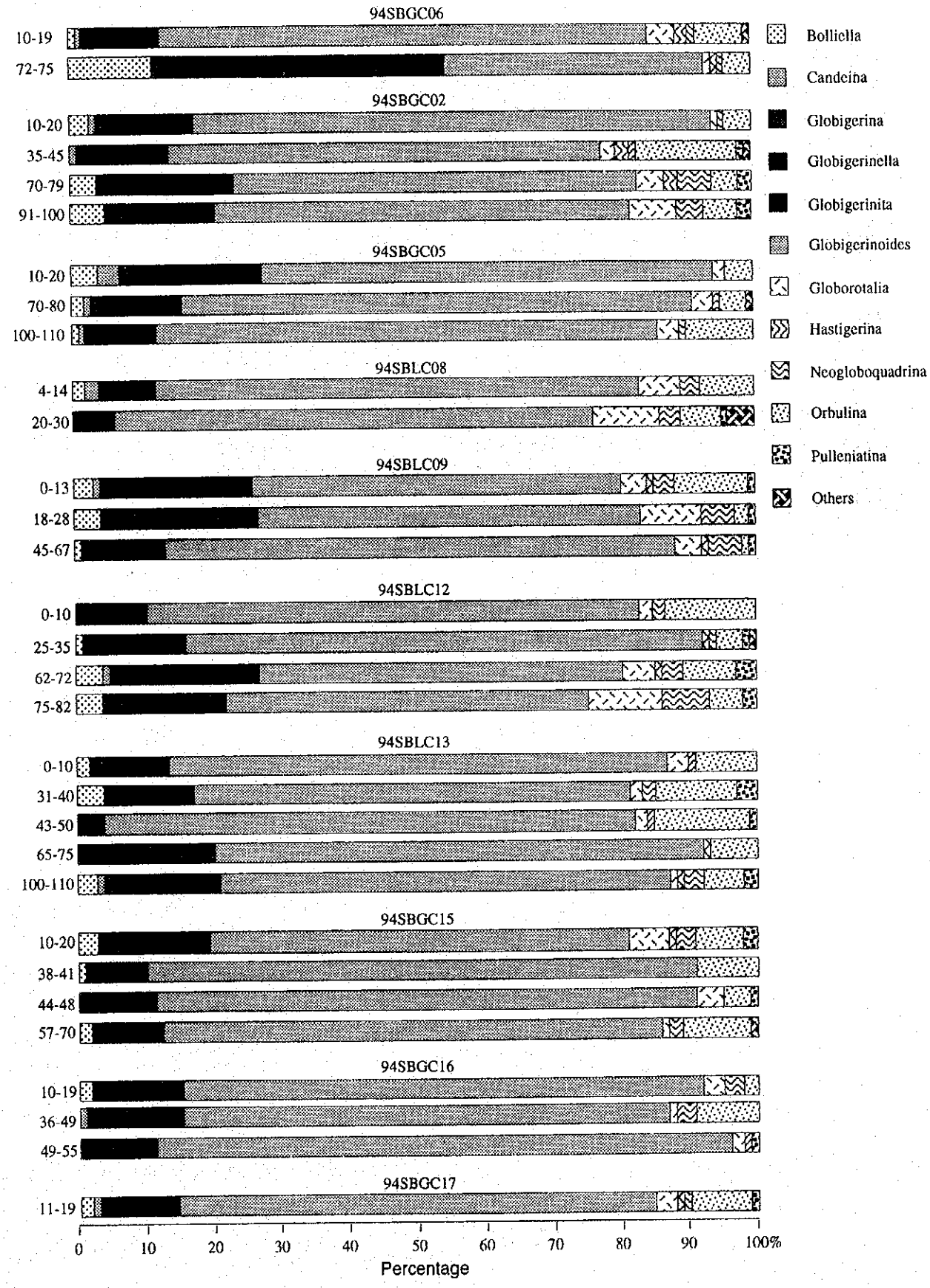

Figure 4-2-5 Abundance of each genus of planktonic foraminifera from the studied cores (1)

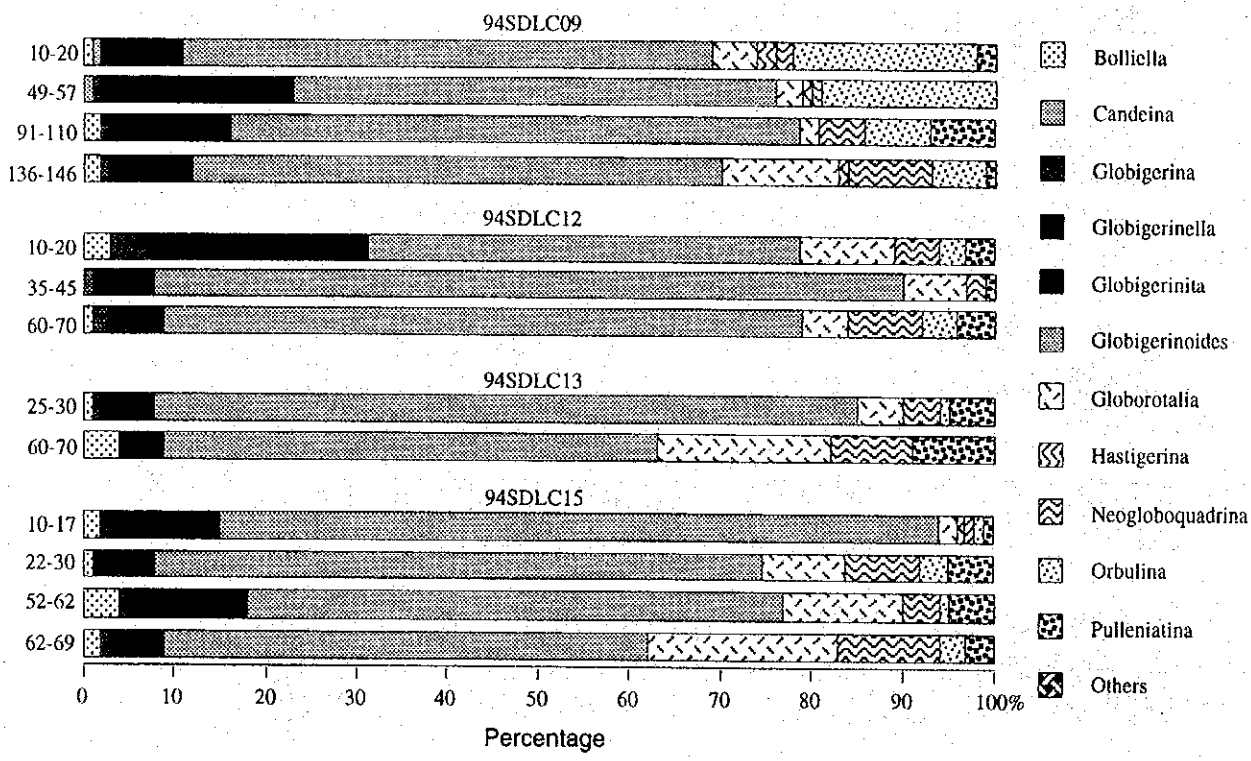

Figure 4-2-5 Abundance of each genus of planktonic foraminifera from the studied cores (2)

We identified 48 species of 14 genera from planktonic foraminifera contained in 44 samples from 14 cores. Generally, the *Globigerinoides* genus account for 50~70% of all planktonic foraminifera, but each of the *Globigerinita, Orbulina, Globigerinella, Globorotalia* and *Neogloquadrina* genera also accounts for more than 10% at times (Figs. 2 and 3). The *Globigerinoides* genus is composed of the *G. ruber* group (*G. rubber, G. elongatus* and *G. pyramidalis), G. sacculifer* group (*G. immaturus* and *G. sacculifer)* and *G. conglobatus.* Among them, both the *G. ruber* group and *G. sacculifer* group occur at frequencies of 10~ 40%, the highest occurrence. But, in most cases, the *G. ruber* group is prominent. *G. conglobatus* account for about 10% of all communities in each sample. Among the *Globorotalia* genus, the *Globorotalia* crassaformis group (crassaformis, viola and ronda) occurs relatively abundantly (about 5%). The *Globigerinella* genus is composed of G. aequilateralis only and the *Globigerinita* genus is *G. glutinata* only. These generally occur at a frequency of about 5 ~ 10%. The Orbulina genus and the Neogloboquadrina genus are composed of 2-3 species respectively, but *O. universa* (generally 5 ~ 10%) and *N. dutertrei* (generally less than 5%) command a majority in each of them. Both the *Bolliella* and *Pulleniatina* genera are used as index species for determing geological age but the frequency of them is generally as low as 5%. Other genera are also less than 5%.

Following is an estimate of the sedimentary environment. From the facts that the planktonic foraminifera fossil group found in the analytic samples are mainly composed of the *Globigerinoides* genus and contain only few of the *Globorotalia truncatulinoides, G. inflata* and *Globigerina bulloides* that occur in horse latitudes, it is inferred that the communities indicate the geographic districts from the tropics to the subtropics.

As previously stated, for the *Globigerinoides* genus, *G. ruber* is prominent in most cases. According to Bé (1977), this species shows a relatively high occurrence from approximately 45° N.L. to 45° S.L., but, if anything, the subtropics are rich in this species. Furthermore, *G. Conglobatus, G.aequilateralis* and *O. universa* occur relatively abundantly in the sediments collected from the survey area and it is well known that these species

occur primarily in the subtropics rather than the tropics (Bé., 1977).

The area from which the analytical samples are collected is classified as the subtropics when viewing from the existing planktonic foraminifera, and the communities in the samples are close to those of the subtropics rather than the tropics. So, it does not contradict.

Now we will examine the rate of sedimentation. For the purpose of examining the rate of sedimentation, we divided the sediments into two groups: one from track line 94SBGC02 to track line 94SDLC17 and the other from 94SDLC09 to 94SDLC15. It is inferred that particles of pyroclastic materials (from silt to pebble-sized) were supplied to sediments of both regions from their hinterlands. Thus, the rate of sedimentation is considerably high as compared with ooze. However, sediments of the former (from 94SBGC02 to 94SDLC17) are rich in pyroclastic particles but sediments of the latter (from 94SDLC09 to 94SDLC15) are considerably less rich in pyroclastic particles. In the case of track lines from 94SBGC02 to 94SDLC17, sedimentation in the *Bo. adamsi* subzone is at the high rate of 35 ~ 45mm/ka, in the *Pu. finalis* subzone at the rate of 2.5 ~ 11mm/ka (mostly at less than 5mm/ka) and in the *Bo. calida calida* subzone at the rate of 0.4 ~ 1.8mm/ka. They show a tendency for the rates of sedimentation to decrease toward the lower horizons.

The *Gr. crassaformis hessi* subzone shows a rate of 0.8mm/ka. The same applies to the cores of 94SDLC09 ~ 94SDLC15, in which sedimentation in the *Bo. adamsi* subzone is at the rate of 17mm/ka, in the *Pu. finalis* subzone at 7 ~ 13.6mm/ka, in the *Bo. calida calida* subzone at 0.5 ~ 1.8mm/ka. The rates become smaller toward the lower horizons. Accordingly, we can say that rates of sedimentation in the past were slower, becaming faster as they approached the present time. The sediments containing pyroclastic materials in the *Bo. adamisi* (from 94SBGC02 to 94SDLC17) show nearly twice as high a rate of sedimentation as the sediments poor in pyroclastic materials (from 94SDLC09 to 94SDLC15). In contrast with this, sediments without pyroclstic materials in the *Pu. finalis* zone have higher rates of sedimentation but sediments in the *Bo. calida calida* zone have almost constant rates. From these we can see that there are some differences in the rate of sedimentation from the *Pu. finalis* subzone to the *Bo. adamsi* subzone in both regions.

(Benthic Foraminifera)

Individuals of benthic foraminiferan community presumed to be resedimented from the shallow seas of continental shelves (the *Quinqueloculina* genus and *Pyrgo* genus) are frequently identified in the sediments of the track lines from 94SBGC02 to 94SDLC17. Some of the communities coexisting with them are composed of species characterizing the zones from the lower layers of the mid-bathyal zone (about 800-2,500m) to the lower bathyal zone (about 2,000-3,500m) (Ingle, 1980, Akimoto・Hasegawa, 1989). And others are coexisting with communities with thin shells like *Chilostomella oolina* and *Bolivinita quadrilatera*.The communities in the latter case may be indicating they were in a lowly oxygenated state.

Conspicuous changes are not recognized from the viewpoint of stratigraphy even in the surface layer.

Genera with agglutinative shells like *Egerella, Trochammina* and *Haplophragmoides* are identified occasionally. On the other hand, individuals of benthic foraminiferan community presumed to be resedimented from the shallow seas of continental shelves (the *Quinqueloculina* genus, *Pyrgo* genus, *Hanzawaia* genus and *Hoeglundina elegans*) are frequently identified in the sediments of the track lines from 94SDLC09 to 94SDLC15. Generally, such resedimented communities are concomitant with agglutinative species (*Egerella bradyi* and *Trochammina sp.*) and the species of the lower bathyal zone (*Pullenia bulloides* and *Nelonis pompuloides*).

From the above, it is considered that the benthic foraminiferan communities found in the samples of this survey area indicate depths of around the lower bathyal zone and that they also indicate that communities sedimented on continental shelves in shallow seas had been frequently carried into this region and resedimented there. As previously stated, some of the sediments containing pyroclastic materials are presumed to have originated from turbidite, so these resedimented communities can be inferred as having the same origin.

<Measurement of grain size distribution of lutaceous substances>

To estimate the sedimentary environment of sediments, we conducted measurements of grain size distribution on constituent grains of lutaceous substances. Measured samples include, as in the above case of identifying microfossils, those collected for the baseline geochemical survey and the ore deposit investigation conducted in the

vicinity of the baseline survey. A totalof 21 samples were measured, 19 samples collected at 9 baseline points and 2 samples collected at 2 points for the ore deposit investigation.

The measurement of grain size distribution was conducted by the JIS 1202-1990 "Test method for soil grains." First, the mass of bottom material samples was measured. Then, samples were washed with water on a 75μm sieve. The substances remaining on the sieve were dried by an oven. Dried substances were submitted to screen analysis. Grain sizes of soil grains under 75μm were measured by sedimentation particle size analysis.

Grain size distribution was measured by the screening method and sedimentation particle size analysis. In order to obtain the grain size distribution of finer-grained particles from the grain sizes cumulative curves, cumulative frequency distribution was plotted on a logarithmic probability paper and logarithmic normal distribution was assumed for the grain size analysis.

Each percentile grain diameter necessary for the calculation was read by the illustrated method and shown in a histogram (Figure 4-2-6) as well as converted into a ϕ scale. Then, median diameters, mean diameters and sorting indexes were obtained by the expressions of Folk & Ward (1957). The results shown in Table 4-2-3. The calculation of sorting indexes by this method, however, is usually used for grain size analysis of sandstone and is not so generally applied to superfine bottom materials like these samples.

The expressions of Folk & Ward (1957) for obtaining coefficients of grain sizes and the assessment of sorting indexes are shown below:

Median diameter $Md\phi = \phi_{50}$

Mean diameter $Mz = (\phi_{16} + \phi_{50} + \phi_{74})/3$

Sorting index $\sigma I = (\phi_{84} - \phi_{16})/4 + (\phi_{95} - \phi_{5})/6.6$

<0.35	: very well sorted
0.35 ~ 0.50	: well sorted
0.50 ~ 0.71	: moderately well sorted
0.71 ~ 1.00	: moderately sorted
1.00 ~ 2.00	: poorly sorted
2.00 ~ 4.00	: very poorly sorted
>4.00	: extremely poorly sorted

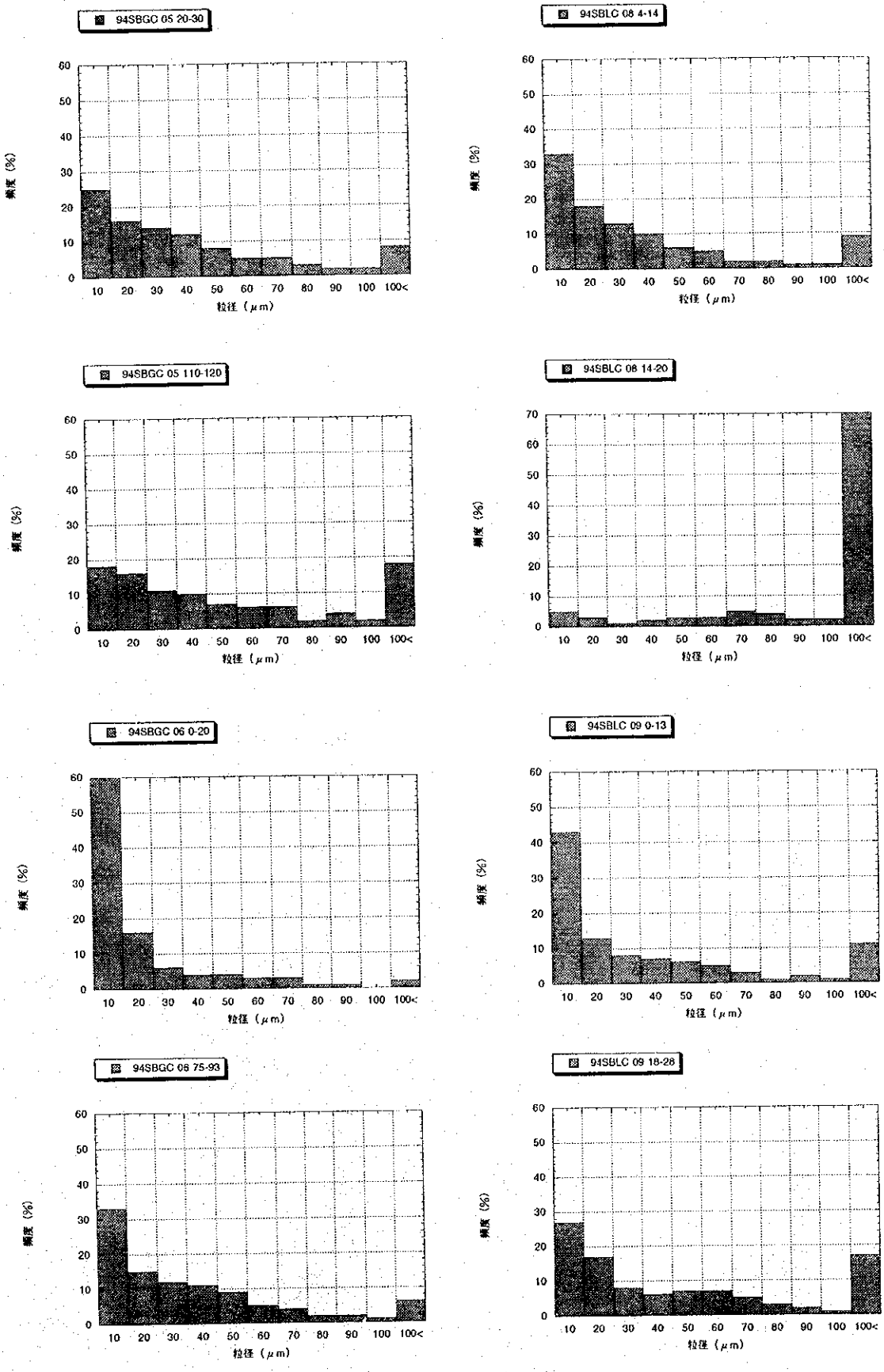

Figure 4-2-6 Histogram of grain size (1)

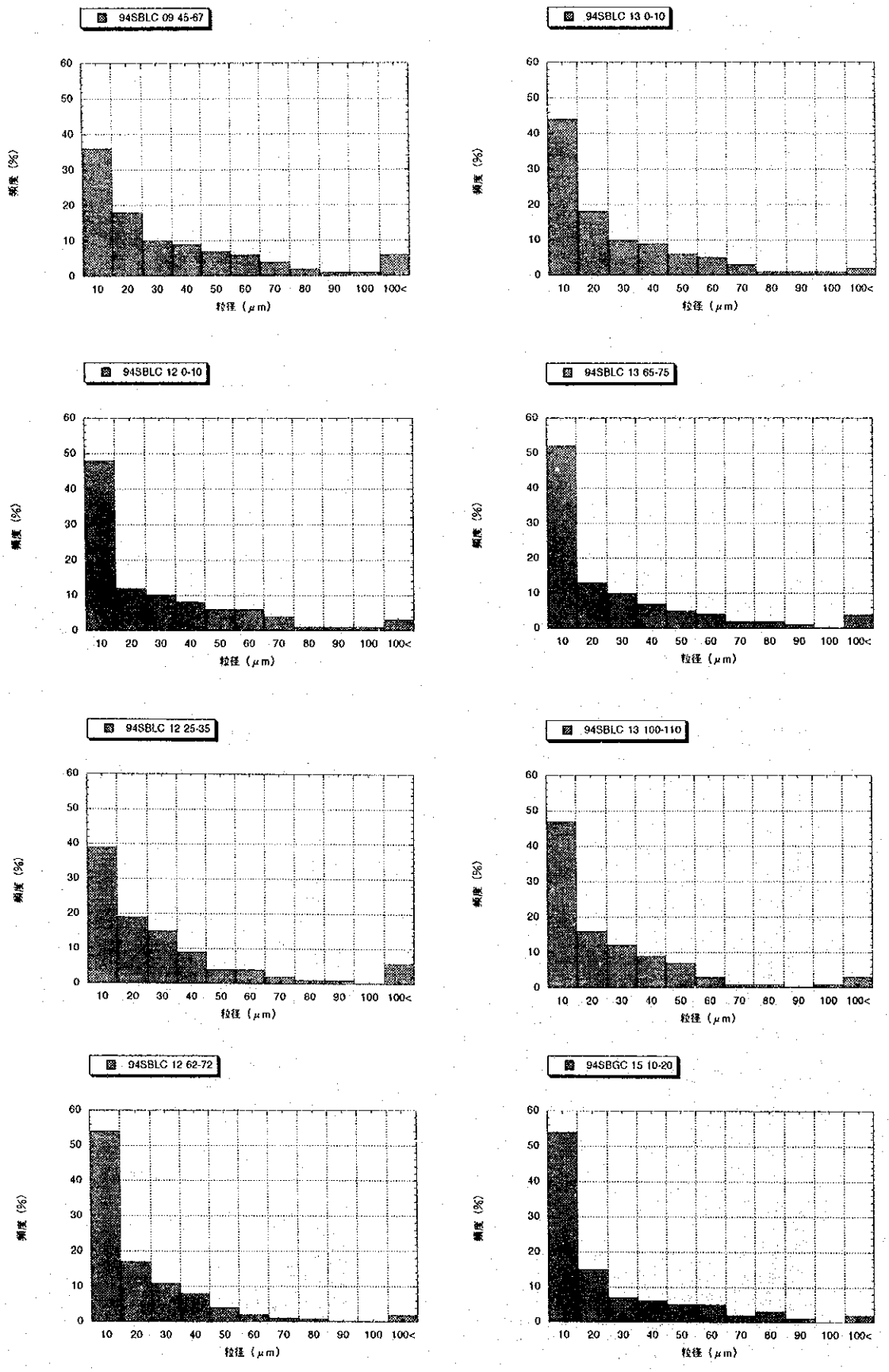

Figure 4-2-6 Histogram of grain size (2)

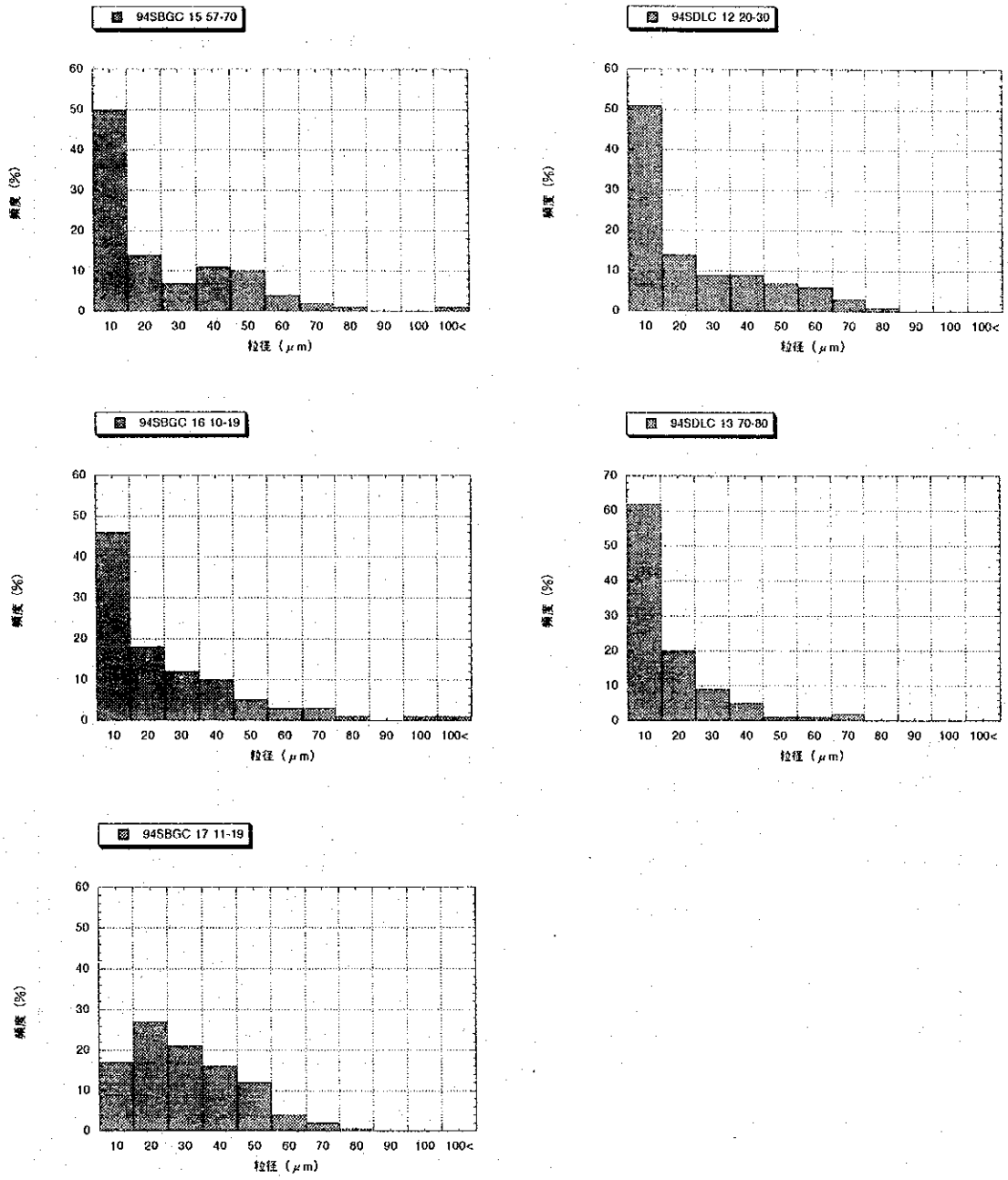

Figure 4-2-6 Histogram of grain size (3)

Table 4-2-3 Results of mechanical analysis of sediments

Sample No.	median diameter (μm)	mean diameter (μm)	sorting coefficient	density (g/cm^3)
94SBGC05 20-30	25.30	18.24	2.39	2.636
94SBGC05 110-120	33.70	31.30	2.18	2.628
94SBGC06 0-20	7.20	4.16	3.47	2.695
94SBGC06 75-93	22.10	14.57	2.70	2.629
94SBLC08 4-14	19.20	13.21	2.62	2.686
94SBLC08 14-20	192.00	188.71	1.98	2.598
94SBLC09 0-13	14.00	5.28	4.62	2.718
94SBLC09 18-28	27.40	26.11	2.50	2.721
94SBLC09 45-67	16.30	12.51	2.71	2.777
94SBLC12 0-10	10.90	4.24	4.06	2.687
94SBLC12 25-35	14.70	11.37	2.41	2.752
94SBLC12 62-72	8.70	3.74	3.71	2.698
94SBLC13 0-10	18.50	6.88	3.48	2.708
94SBLC13 65-75	13.30	3.60	4.77	2.782
94SBGC13 100-100	11.20	7.65	3.62	2.681
94SBGC15 10-20	8.30	1.18	3.87	2.7
94SBGC15 57-70	10.00	2.00	5.50	2.647
94SBGC16 10-19	11.30	6.09	3.24	2.688
94SBGL17 11-19	22.80	20.17	1.47	2.648
94SDLC12 20-30	9.50	2.25	4.49	2.682
94SDLC13 70-80	6.60	1.88	4.24	2.677

Characteristics of grain size distribution classified by each sampling point are as follows:

In the case of superfine samples, the width of grain diameter's ϕ values become very wide, so the sorting index for each sample becomes large (poor). The method of calculation suggested by Folk & Ward (1957) is mainly used for the grain size assessment of sandstone and it remains to be a subject of discussion whether we can use it for these samples that are rich in fine grains.

Furthermore, it is difficult to estimate their palaeoenviroment only from the grain size analysis of superfine bottom sediments. Observation of coarse-grained substances contained in bottom sediments (determining whether they are terrigenous clastics or not) and discussion of microfossils contained in bottom sediments are also required.

- 94SBGC05 (2 samples)

This core's median diameters are 25.3 $\sim$ 33.7μm and mean diameters are 18.2 $\sim$ 31.3μm. Both of them indicate the grain sizes of silt. Its sorting indexes are 2.18 $\sim$ 2.39. In the frequency distribution charts, both samples have their peaks at grain diameters of 10 $\sim$ 30μm. Particles larger than 100μm are richer at depths of 110-120cm, which account for 18%.

Grain size cumulative curves show that grain sizes will be a little bit larger than 20-30cm at depths of 110-120cm but, on the whole, they have similar curves, from which, it is inferred that the sedimentary environment had undergone little change.

- 94SBGC06 (2 samples)

This core's median diameters are 7.2 $\sim$ 22.1μm and mean diameters are 4.16 $\sim$ 14.57μm. Both indicate the grain sizes of silt. Sorting indexes are 2.70 $\sim$ 3.47. In the frequency distribution charts, both samples have their peaks at grain diameters of 10 $\sim$ 20μm. Grain size cumulative curves show that grain sizes will be larger than 0-20cm at depths of 75-93cm. It can be said that the sediments changed to finer grains at depths of 0-20cm.

- 94SBLC08 (2 samples)

This core's median diameters are 19.2 ~ 192.0μm and mean diameters are 13.21 ~ 188.71μm. They differ among samples and indicate the grain sizes of silt and fine sand. Sorting indexes are 1.98 ~ 2.62.

In the frequency distribution charts, the samples show totally different frequency distribution at two depths. Silt and clay account for 88% at depths of 4-14cm but they account for only 25% at depths of 14-20%, in which sand commands a majority, a distinguishing characteristic as compared with samples from other cores. From this, we consider that sources of sediment supply and sedimentary environment changed greatly at depths of 4-14cm and 14-20cm.

- 94SBLC09 (3 samples)

This core's median diameters are 10.9 ~ 27.4μm and mean diameters are 5.28 ~ 26.11μm. They vary little among samples and indicate the grain sizes of micro-grained silt. Sorting indexes are 2.5 ~ 4.62.

Every sample shows similar patterns in frequency distribution charts. Facies of these sediments vary little, so we consider that they compose roughly the same horizon.

- 94SBLC12 (3 samples)

This core's median diameters are 8.7 ~ 14.7μm and mean diameters are 3.74 ~ 11.37μm. They vary little among samples and indicate the grain sizes of micro-grained ~ fine-grained silt. Its sorting indexes are 2.41 ~ 4.06.

Patterns of frequency distribution charts bear close resemblance. Facies of theses ediments vary little, so we consider that they compose roughly the same horizon.

- 94SBLC13 (3 samples)

This core's median diameters are 11.2 ~ 18.5μm and mean diameters are 3.60 ~ 7.65μm. They vary little among samples and indicate the grain sizes of micro-grained~fine-grained silt. Sorting indexes are 2.41 ~ 0.06.

Patterns of frequency distribution charts bear very close resemblance. Facies of these sediments vary little, so we consider that they compose roughly the same horizon.

- 94SBGC15 (2 samples)

This core's median diameters are 8.3 ~ 10.0 μm and mean diameters are 1.18 ~ 2.00 μm. Both samples have little dispersion and indicate the grain sizes of micro-grained ~ fine grained silt. Sorting indexes are 3.87 ~ 5.50.

Patterns of frequency distribution charts bear very close resemblance. Facies of these sediments vary little, so we consider that they compose roughly the same horizon.

- 94SBGC16 (1 sample)

This core's median diameter is 11.3 μm and mean diameter is 6.09 μm. Its sorting index is 3.24.

Patterns of the frequency distribution chart are harmonious with samples from other cores, so we consider it was in a similar sedimentary environment.

- 94SBGC17 (1 sample)

This core's median diameter is 22.8 μm and mean diameter is 20.17 μm. Its sorting index is 1.47. The distinguishing characteristics of this sample are low in clay as compared with samples of other cores and silt accounts for 88%. This can be identified by patterns of the frequency distribution chart. So, we consider it was in a different sedimentary environment from samples of other cores.

- 94SDLC12 (1 sample)

This core's median diameter is 9.5 μm and mean diameter is 2.25 μm. Its sorting index is 4.49. Its grain sizes are 59% of silt and 41% of clay, which indicates that this core is rich in fine-grained components.

Patterns of the frequency distribution chart resemble the grain size distribution of 94SDLC13, though this sample is richer in grains larger than 40 μm as compared with 94SDLC13.

- 94SDLC13 (1 sample)

This core's median diameter is 6.6 μm and mean diameter is 1.88 μm. Its sorting index is 4.24. Silt accounts for 55% and clay accounts for 45% in this sample. This sample is most rich in fine-grained components among all samples.

A high percentage of fine-grained components can be identified even from the

patterns of the frequency distribution chart. From this, we can consider that terrigenous sediments had participated only slightly in this sedimentary environment.

<The results of microscopic observation on volcanic sand>

As previously stated, sand is abundantly distributed among muddy substances of the samples collected during the baseline geochemical survey. With the object of identifying constituent minerals of the sand and estimating the sedimentary environment of the survey area, we conducted thin section appraisal in parallel with the identification of microfossils.

8 samples from 7 points, in which conspicuous sand was observed, were selected from samples of bottom materials collected from 10 points during the baseline survey. As the samples were fragile, they were sealed in resin and cut into thin sections.

As the result of appraisal, most of the rock fragments are found to be of basic volcanic rock origin, and iron hydroxide fragments and foraminiferan remains are recognized. Rock fragments are composed of non-porphyritic basait, augite basalt ~ andesite, augite basalt containing hypersthene, hypersthene augite basalt, pumice and scoria.

The basalt ~ andesite fragments assume the internal texture, hyalopilitic texture and vitric texture.

The details of the results of appraisal, described in order from the northeastern side of the baseline sampling points, are as follows;

Typical microphotographs are shown in Figure 4-2-7 and the results of observation are shown in the Appendix Table 7.

- 94SBGC06

This sample is basaltic clastics distributed between 30cm and 36cm below the surface layer of 94SBGC06. Macroscopically it appears dark gray and is rich in scoria.

Microscopically, plagioclase is observed in addition to scoria, with small amounts of augite hypersthene, olivine and magnetite apatite, Mn oxides and Fe oxides are observed. They are not altered.

Plagioclase assumes idiomorphic of 0.1mm ~ 1.5mm and is observed rarely. Augite, hypersthene, magnetite and apatite also appear idiomorphic and the sizes of phenocryst are 0.1mm ~ 1.0mm. Especially, polysynthetic twin and zonal structure

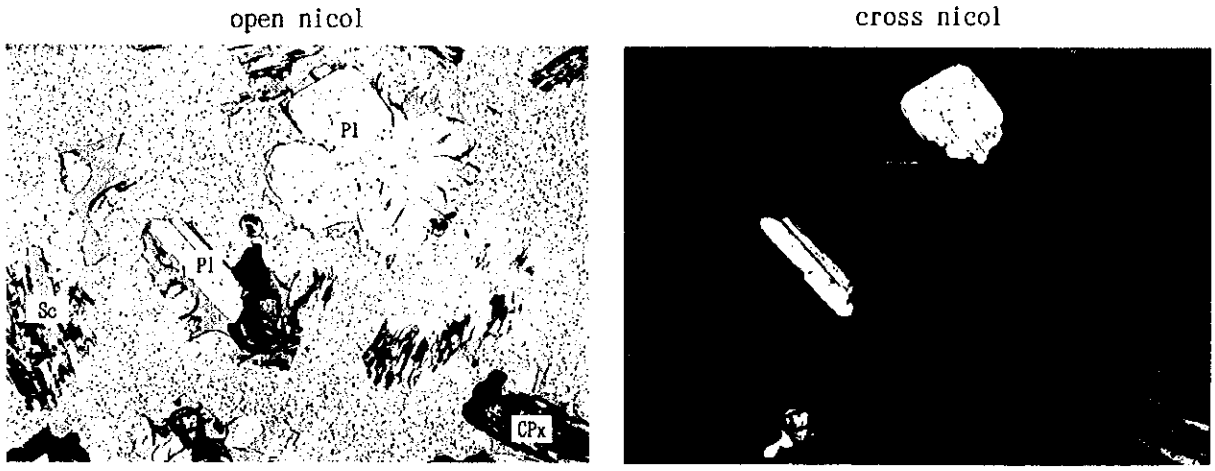

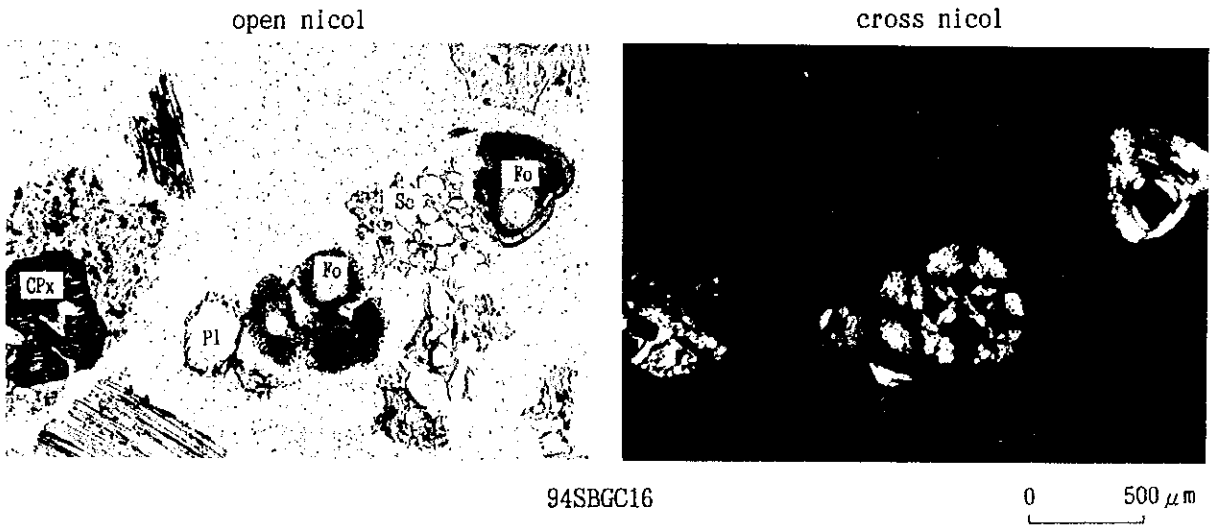

Abbreviation

Fo : Foraminifera
Gℓ : Glass
Iℓ : Ilmenite
Mt : Magnetite
Pℓ : Plagioclase
Px : Pyroxene
CPx : Clinopyroxene
OPx : Orthopyroxene
Sc : Scoria

Figure 4-2-7 Microscopic Photos of Volcanic Sand (Baseline Geochemcal Survey)

are clearly observed in augite.

Olivine exibits granular structurec of about 0.3mm size. Mn oxides and Fe oxides assume polymorphism of 0.2mm ~ 0.8mm (their external forms are indeterminate). Scoria assumes polymorphism of 0.5 ~ 1.8mm and vesicles caused by vesiculation are prominent.

- 94SBGC02

This sample is basaltic clastics distributed between 21 ~ 24cm below the surface layer of 94SBGC02. Macroscopically, it appears, as in the case of 94SBGC06, dark gray.

Microscopically, it is abundant in plagioclase and scoria, and a moderate amount of pyroxene basalt fragments (maximum diameter of 3mm) are observed. Foraminiferan shells are also observed, though only a few.

Plagioclase and augite of about 0.3 ~ 0.8mm sizes are observed in the phenocrysts of pyroxene basalt fragments and an intersertal texture is observed in their matrices.

Scoria is observed abundantly and its volume ranks first in this sample. Their major axes are 0.5 ~ 4mm and vesicles caused by vesiculation are prominent. It is considered to be light brown mafic magma origin.

Among mineral particles, plagioclase is most abundantly observed. A moderate amount of augite, Fe-Mn oxides and a small amount of hypersthene, magnetite and apatite are observed.

- 94SBLC08

This sample is basaltic clastics distributed between 20 ~ 42cm below the surface layer of 94SBLC08. Macroscopically, it appears dark gray.

Microscopically, a number of rock fragments are observed. Especially, it is rich in subangular pebble ~ rounded pebble non-porphyritic basalt fragments of 2 ~ 4mm sizes. 2.5mm ±sized rubble ~ subpebble augite andesite containing hypersthene fragments, subangular pebble basalt fragments and Fe hydroxides with inclusion of small rock fragments are also observed in small amounts. Scoria, with the maximum size of 7mm, is also observed abundantly.

Plagioclase and augite > hypersthene are recognized in the phenocrysts of augite andesite fragments. An interserta texture is recognized in their matrices.

The hydropilitic texture is recognized in the matrix of non-porphyritic basalt.

On the other hand, such mineral particles as plagioclase of 0.1 ~ 2.5mm sizes, augite, magnetite and hypersthene of about 0.1 ~ 0.6mm sizes are observed. They assume idiomorophic ~ hypidiomorphic characteristics. A trace quantity of hypersthene is also observed. Quantitatively, plagioclase ranks first, followed by augite and magnetite. A trace quantity of hypersthene is observed.

- 94SBLC09

This sample is distributed from 14 ~ 15cm (upper layer) to 38 ~ 40cm (lower layer) below the surface layer of 94SBLC09. It is volcanic detritus. The upper layer appears basaltic and the lower layer andesite ~ basaltic.

Microscopically, fragments of augite basalt containing hypersthene, augite basalt ~ andesite, augite basalt and non-porphritic basalt are observed in the upper layer. Rock fragments of augite andesite containing hypersthene, augite basalt, and Iron-hydroxides containing small crystals of plagioclase and pyroxene are observed. Plagioclase and others are also observed as mineral particles. Scoria is abundantly observed in the lower layer.

These rock fragments generally appear as rubbles of 2 ~ 7.5mm sizes. Plagioclase, augite, hypersthene and others are observed in their phenocrysts and an intersertal ~ hyalopilitic texture is observed in their matrices.

Plagioclase recognized in the lower layer assume fragmental sizes smaller than 1mm diameter. Unidentified minerals mingled with plagioclase crystals are observed. These unidentified minerals are colorless with relatively high refractive indexes under the parallel nicols but appear dark black under the crossed nicols.

Scoria observed in the lower layer shows conspicuous traces of vesiculation and, occasionally, with inclusion of phenocrysts of plagioclase and augite. Macroscopically, it appears yellowish brown ~ light brown and is inferred as intermediate ~ mafic magma origin.

- 94SBLC13

This sample is volcanic detritus distributed between 31 ~ 40cm below the surface layer. The same detritus are distributed above this sample from 23 ~ 25cm (upper part) to 25 ~ 31cm (middle part) below the surface layer. This sample corresponds to the lower layer of such detritus.

Macroscopically, it appears to be dark gray pumice of 20±cm diameter and scoria of 13cm diameter.

Microscopically, the phenocryst of pumice is composed of plagioclase, augite and hypersthene. Its matrix is composed of nearly colorless vesicular glass. It is inferred to be of intermediate igneous rock origin.

On the other hand, the phenocryst of scoria is composed of plagioclase and augite. Its matrix is composed of light brown vesicular glass. It is inferred to be of mafic magma origin.

- 94SBLC15

This sample is basaltic clastics distributed between 28 ~ 29cm below the surface layer. Macroscopically, it appears dark gray.

Microscopically, pyroxene basalt and non-porphyritic basalt are observed in rock fragments, and idiomorphic plagioclase, augite, hypersthene, magnetite and apatite as well as Fe-Mn oxides with indeterminate external forms are observed in mineral particles. Abundant scoria with indeterminate external forms and a moderate ~ small amount of foraminiferan shells are also observed.

Pyroxene basalt is composed of rubble ~ subrubble rock fragments with 0.6 ~ 1.8mm diameters. Its phenocryst is composed of plagioclase and augite and its matrix indicates the vitric ~ hyalopilitic texture.

Non-porphyritic basalt is composed of 1mm± rubble and its matrix indicates the vitric ~ hyalopilitic texture.

Plagioclase is most abundantly recognized among mineral particles and polysynthetic twins are clearly observed. As for the sizes of particles, plagioclase has major axes of 0.2 ~ 2.5mm and other minerals of about 0.1 ~ 1.5mm. Most of the minerals are contained in scoria.

Scoria show many traces of vesiculation. Glass appears light brown. The origin of scoria is inferred as mafic magma.

- 94SBLC16

This sample is basaltic clastics distributed between 32 ~ 33cm below the surface layer. Macroscopically, it appears dark gray.

Microscopically, non-porphyritic basalt is observed in rock fragments and

idiomorphic plagioclase, augite, hypersthene, magnetite and apatite are recognized in mineral particles. Abundant scoria with indeterminate external forms and a moderate ～ small amount of foraminiferan shells are also observed.

Non-porphyritic basalt is composed of rubble with diameters of 0.6 ～ 2mm± and its phenocryst is composed of a small amount of plagioclase. Its matrix indicates the intersertal texture. Some of the non-porphyritic basalt has fine pore spaces indicating subrubble and their matrices indicate the vitric ～ hyalopilitic texture.

Plagioclase is most abundantly recognized among mineral particles and polysynthetic twins are clearly observed. As for the sizes of particles, plagioclase has major axes of 0.2 ～ 2.5mm and other minerals are about 0.1 ～ 0.8mm. Such minerals are often contained in scoria.

On the other hand, scoria show many traces of vesiculation.

Glass appears light brown. The origin of scoria is inferred as mafic magma.

4-3 Results of the Survey

Chemical analysis and powder X-ray diffraction test were conducted on samples of seafloor sediments collected from the survey area.

In addition to the sediments collected during the baseline survey, some of the sediments collected during the ore deposit investigation were analyzed. A list of analyzed samples is shown in the Appendix Table 3.

(1) Chemical analysis

Analytical components and the limits of detection are as follows: SiO_2, TiO_2, Al_2O_3, FeO, MgO, MnO, MgO, CaO, BaO, Na_2O, K_2O, P_2O_5, CO_2, LOI (the limit of detection of above 13 whole rock components is 0.01%), Ag (0.02ppm), Cu (1ppm), Pb (1ppm), Zn (1ppm), Mn (5ppm), Total-S (0.001%), Cd (0.1ppm), Ni(1ppm), Co (1ppm), As (0.2ppm), Sb (0.2ppm), Hg (10ppb), Ba (5ppm), Sr (1ppm), Cl (100ppm), P (0.05%), SO_4 (0.01%), CO_2 (0.1%), Cr (2ppm), V (1ppm), Tl (0.1ppm), B (5ppm), Li (1ppm), Rb (5ppm), U (0.2ppm). Figures and units in the parentheses show the limits of detection.

Methods of analysis for each component are listed below. Results of analysis are shown in the Appendix Table 5.

Analytical Element	Method of Analysis
SiO_2, TiO_2, Al_2O_3, Fe_2O_3, MnO, MgO, CaO, BaO, Na_2O, K_2O, P_2O_5, LOI, Pb	FRF(Fluorescence X-ray Analysis)
Cu, Ni, Co, Ba, Sr, P, Cr, V	ICP Emission Analysis
Ag, Pb, Zn, Cd, As, Sb, Hg	HCl-KClO3 deiestion and extraction
Li, Tl, Ba	A.A.(Atomic Absorption Method)
B, Cl	N.A.A.(Neutron Activation Analysis)
Hg	Cold Vapour A.A.
S, CO_2	LECO-Induction-Furnace
U	Delayed-Neutron-Counting
FeO	Neutralization Titration Method

(2) X-ray Diffraction

Aiming at elucidating the mineral composition of lutaceous (muddy) substances and their quantitative ratio, X-ray diffraction was conducted by a non-oriented method. A total of 99 samples, 56 samples collected from 10 baseline survey points and 43 samples collected from 12 ore deposit investigation points, were tested.

The samples were unsealed, a moderate amount was taken, and air-dried at room temperature. Air-dried samples were crushed under 10μm by a agate · mortar. Samples for testing were press-fitted into aluminum plates carefully so that the diffraction surface would not be oriented. Conditions of X-ray diffraction are as follows:

Unit model : RAD-B Type, made by Rigaku Denki Co., Ltd.
Bulb/Filter : Cu bulb/Ni filter
Voltage/Current for bulb: 30KV/20mA
Scanning angle : 2 ~ 60° (2θ)
Scanning rate : 4° /min.
Paper speed : 4cm/min.
Full scale : 1,000 cps

Minerals identified by the test are semi-quantitatively shown in the Appendix Table 5.

Identified minerals are as follows :

Silicic acid	: quartz, cristobalite
Silicate mineral	: plagioclase, amphibole, hypersthene, augite, analcime, stibite, montmorillonite
Fe-Mn oxide	: magnetite, ilmenite, hematite, goethite, todorokite, birnessite
Carbonate	: calcite, aragonite
Chloride	: rock salt (halite)
Others	: amorphous substances

Quartz was judged by the existence of the strongest ray peak, but due to insufficient peak intensity, it was indeterminable. In the case of cristobalite, its strongest ray overlapped with the peak of plagioclase. As plagioclase coexists with cristobalite in most of the samples, so the existence of cristobalite is indeterminable. In this report, we defined that if cristobalite had an extremely high intensity of the strongest ray peak angle as compared with the strongest ray peak angle of plagioclase, then we determined that cristobalite existed.

We can presume that plagioclase, amphibole, hypersthene and augite are rock-forming minerals for basaltic clastics origin. Analcime and stibite are, in most cases, recognized in relatively lower layers of soft sediments. Montmorillonite is recognized in nearly half of the samples but its mineralogical details are not clear as we have not conducted various processes. Also, in the case of samples with weak peaks, we found difficulty in distinguishing weak peaks from broad peaks of amorphous substances. So, their existence is indeterminable.

We can presume that magnetite and ilmenite are rock-forming minerals of basaltic clastics origin. Hematite, goethite, todorokite and birnessite might be components of manganese oxides.

We can presume that calcite and aragonite are the calcareous remains of foraminiferan shells and others.

Rock salt (halite), which is universally recognized, is inferred to be crystallized from sea water in the soft sediments when the samples were air-dried.

Quantitative ratios of amorphous substances are based on broad rises of 20 ~

40° (2θ) on recording paper. Above- mentioned montmorillonite, goethite, todorokite and birnessite also assume several broad reflexion peaks.

(3) Statistical analysis

We conducted the statistical analysis on the basis of results obtained by the chemical analysis made on 78 samples of seafloor sediments collected from the survey area.

Table 4-3-3-1 shows the maximum, minimum and mean values of the 14 principal components and 25 trace elements.

As shown by these tables, each chemical composition of 78 samples analyzed varies considerably.

LIO accounts for more than 10% in most of the samples. As samples with high-LIO indicate high-CaO value and low-LOI indicates low-CaO, high-LOI is considered to be derived from biogenic origin.

CO_2 accounts for more than 10% in most of the samples in which we have observed abundant foraminiferan shells macroscopically.

As for Ag, Hg and Cd, about half of the samples showed values below the limit of detection.

Table 4-3-3-1 Mean, standard deviation, minimum and maximum of chemical component

Component		Geometric mean	Standard deviation	Maximum	Minimum
SiO2	%	43.88	7.629	54.38	20.14
TiO2	%	0.64	0.177	1.34	0.08
Al2O3	%	13.04	2.930	18.65	1.36
Fe2O3	%	10.12	6.707	45.70	6.22
FeO	%	3.05	1.644	8.89	0.19
MnO	%	0.45	0.463	2.76	0.04
MgO	%	2.88	0.662	5.41	1.22
CaO	%	12.32	5.298	24.42	1.76
BaO	%	0.05	0.017	0.08	0.01
Na2O	%	3.32	0.688	4.52	1.87
K2O	%	1.45	0.675	3.04	0.15
P2O5	%	0.32	0.215	1.76	0.17
CO2	%	5.86	4.727	16.54	0.15
LOI	%	11.58	6.385	24.24	0.18
Total	%	100.05	0.589	101.02	97.91
Ag	ppm	0.03	0.019	0.10	0.02
As	ppm	117.76	638.746	4100.00	0.40
Cu	ppm	86.92	26.393	177.50	0.80
Hg	ppm	96.67	508.146	4550.00	10.00
Pb	ppm	10.35	5.605	31.00	2.00
Sb	ppm	0.86	1.170	5.80	0.20
Zn	ppm	49.33	14.704	88.00	3.00
Ba	ppm	452.44	152.947	690.00	60.00
Cd	ppm	0.55	0.150	1.00	0.50
Co	ppm	23.78	7.794	75.00	1.00
Cr	ppm	27.46	15.714	103.00	6.00
Mn	ppm	2525.73	1626.176	8740.00	120.00
Ni	ppm	16.12	8.030	44.00	3.00
P	ppm	1442.05	974.928	8350.00	710.00
Sr	ppm	579.67	165.784	885.00	117.00
Tl	ppm	0.24	0.254	1.30	0.10
V	ppm	229.00	217.181	1990.00	111.00
Li	ppm	9.83	3.995	31.00	1.00
Cl	ppm	9072.73	1581.848	10000.00	2300.00
B	ppm	48.36	35.712	250.00	15.00
Rb	ppm	19.68	8.230	40.00	7.00
U	ppm	0.98	1.604	14.20	0.20
Total-S	%	0.09	0.080	0.72	0.01
SO4	%	0.07	0.033	0.14	0.01
CO2	%	5.86	4.727	16.54	0.15

Chapter 5. Ore Deposit Investigation

5-1 Outline

No reports have been made on hydrothermal deposits in this survey area, except around Epi Island, and details of submarine topography as well as submarine topographical structure are not known.

Accordingly, we selected sea areas, in which the potential occurrence of hydrothermal deposits could be expected, by conducting acoustic and magnetic surveys.

After areas were selected potential, ore deposit investigation to determine the occurrence of submarine hydrothermal deposits.

In selecting the survey area, we utilized the bathymetric map, acoustic image map and magnetic anomaly map established on the basis of the acoustic and magnetic surveys and others as we described in Chapter 3, and considered

① topography of ridges and sea knolls in the back arc,

② seamounts concomitant with tectonic lines and seamounts with craters in the neighborhood of volcanic fronts,

③ outcrop regions or regions with magnetic anomalies suggesting the existence of new volcanism.

Thus, the following 5 sea areas (Fig. 5-1-1) were selected. Details of the areas are as follows:

1) 94S01 Seamount

From the bathymetric map, we know that this is a seamount with a caldera in its central part, located directly above the intersection of a prominent tectonic line trending NW-SE and a tectonic line orthogonalizing it. This seamount also indicates conspicuous magnetic anomalies.

This seamount has a major axis of about 20km, a minor axis of about 8km and a relative height of about 1,000m. Its top is at water depths of about 1,100m and the caldera in its central part has a major axis of 3km and a minor axis of 2.5km.

Figure 5-1-2 shows the bathymetric map of this seamount.

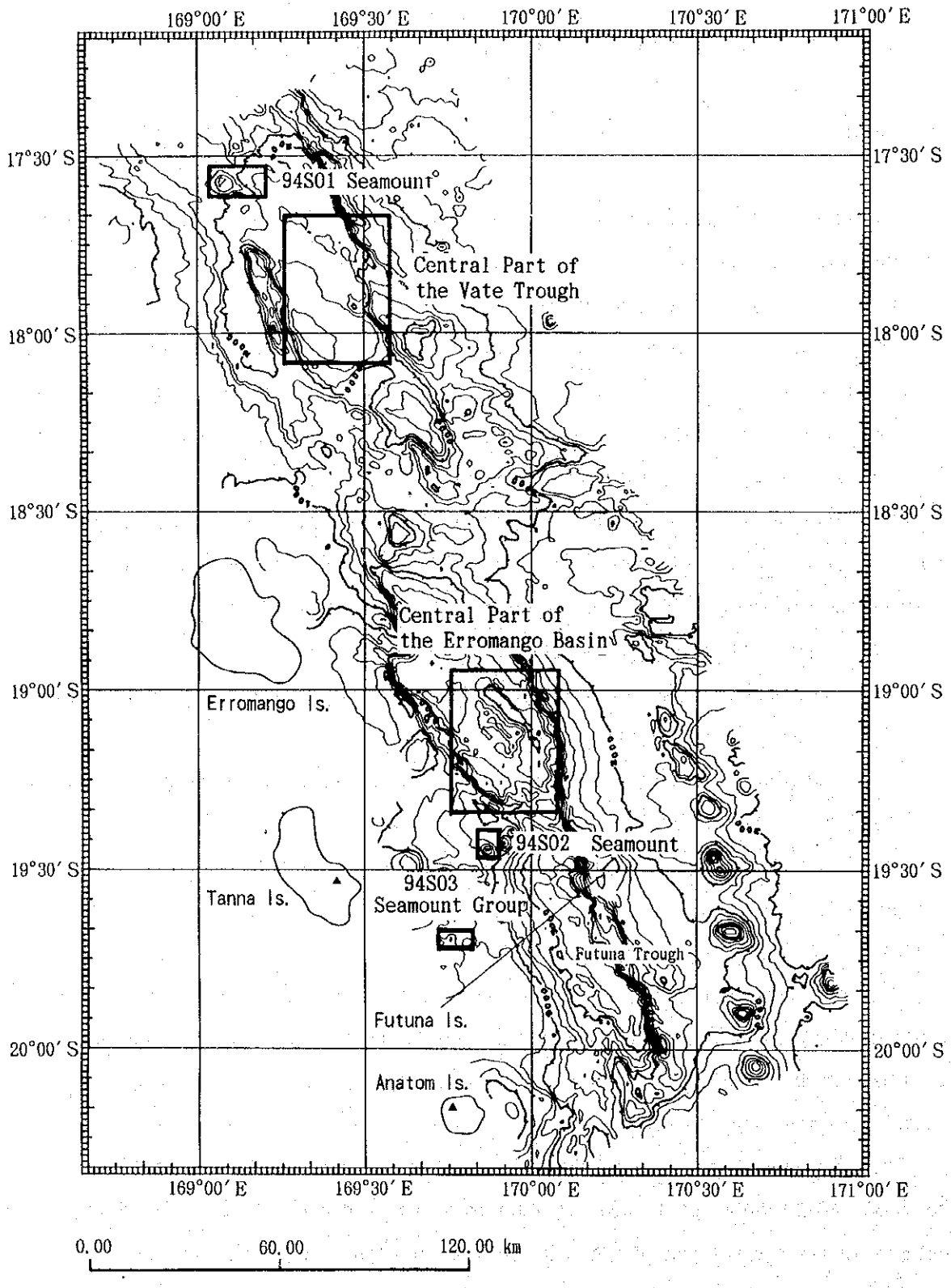

Figure 5-1-1 Location Map of the Ore Deposit Investigation

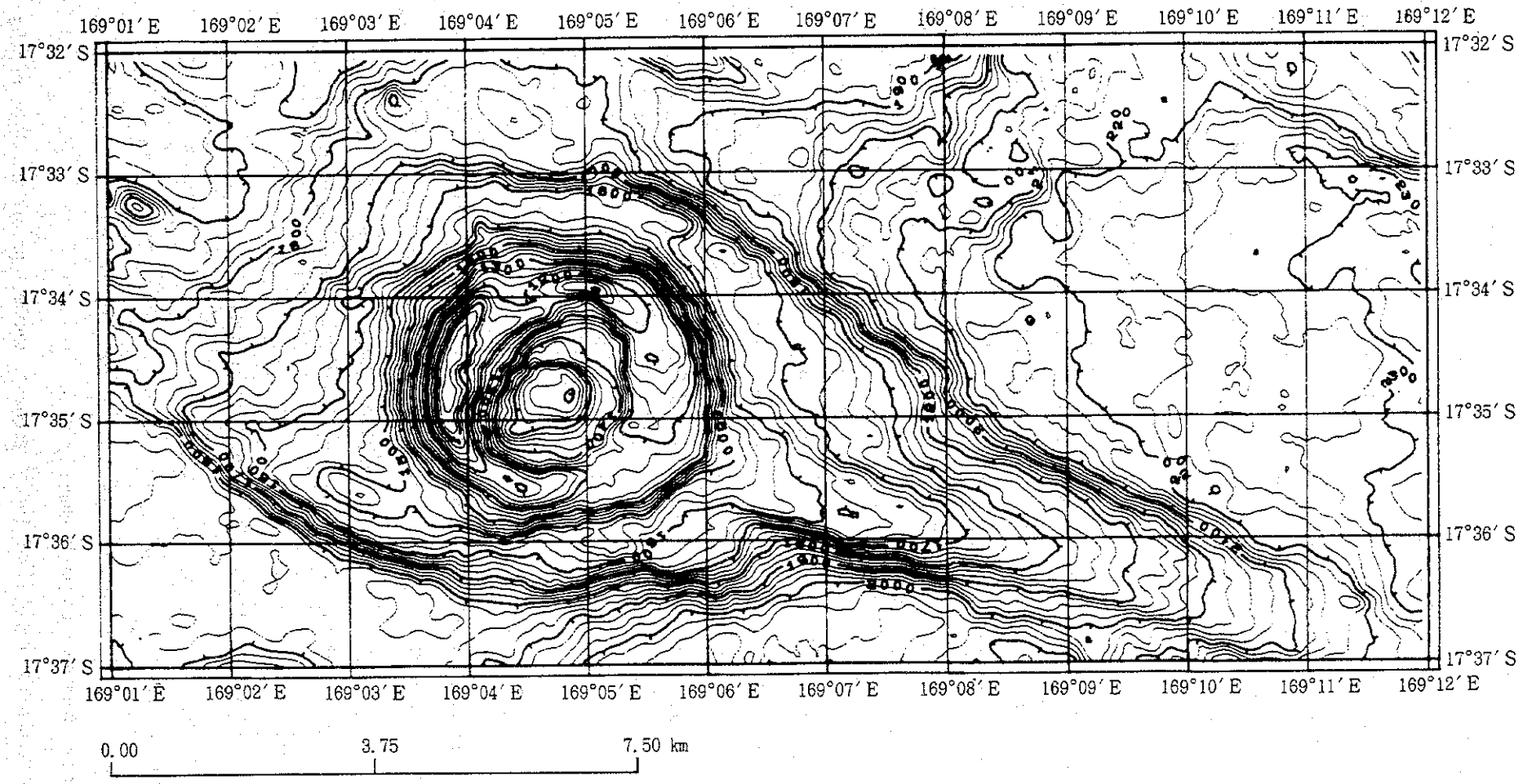

Figure 5-1-2 Bathymetric Map (94S01 Seamount)

2) Central part of the Vate Trough

This is inferred from the sound pressure chart as a sea area with a high potential of new magma activity due to indications of a high potential of outcropped rock masses and magnetic anomalies.

As a topographic feature, a weak ridge topography affected by a NW-SE trending structural control is recognized in the northern part. This ridge continues from the 94S01 seamount.

3) Central part of the Erromango Basin

The existence of a relatively prominent ridge-graben is recognized from the bathymetric chart. From its morphology, it is inferred there is high probability that this is the spreading part of the trough.

As described in Chapter 3, the central ridge is a prominent formation. Its major axis is about 20km and minor axis is about 6km. Water depth is about 2,200m and its trend is N44° W. A northern ridge is distributed on the north side of the central ridge and a graben lies between the central and north ridges. Water depths of this graben are more than 3,000m and the relative height of this graben with the ridges is about 1,000m. Furthermore, the existence of a small-scale southern ridge is recognized on the south side of the central ridge. But the graben lying between the central and southern ridges is underdeveloped.

Figure 5-1-3 shows the bathymetric chart of this sea area.

4) 94S02 seamount

Located between the Erromango Basin and the Futuna Trough, this belongs to a chain of seamounts on an NE-SW trending tectonic line that passes the sill of the Erromango Basin and the Futuna Trough. Its relative height is about 1,000m.

It is a conical seamount with a diameter of about 5km and assumes a small crater topography on the top.

Figure 5-1-4 shows the bathymetric chart of this seamount.

5) The 94S03 seamount group

This is a seamount group arrayed in the direction of EW, in the vicinity of a volcanic front and a prominent magnetic anomaly zone.

This seamount group is composed of three seamounts whose tops are at water depths

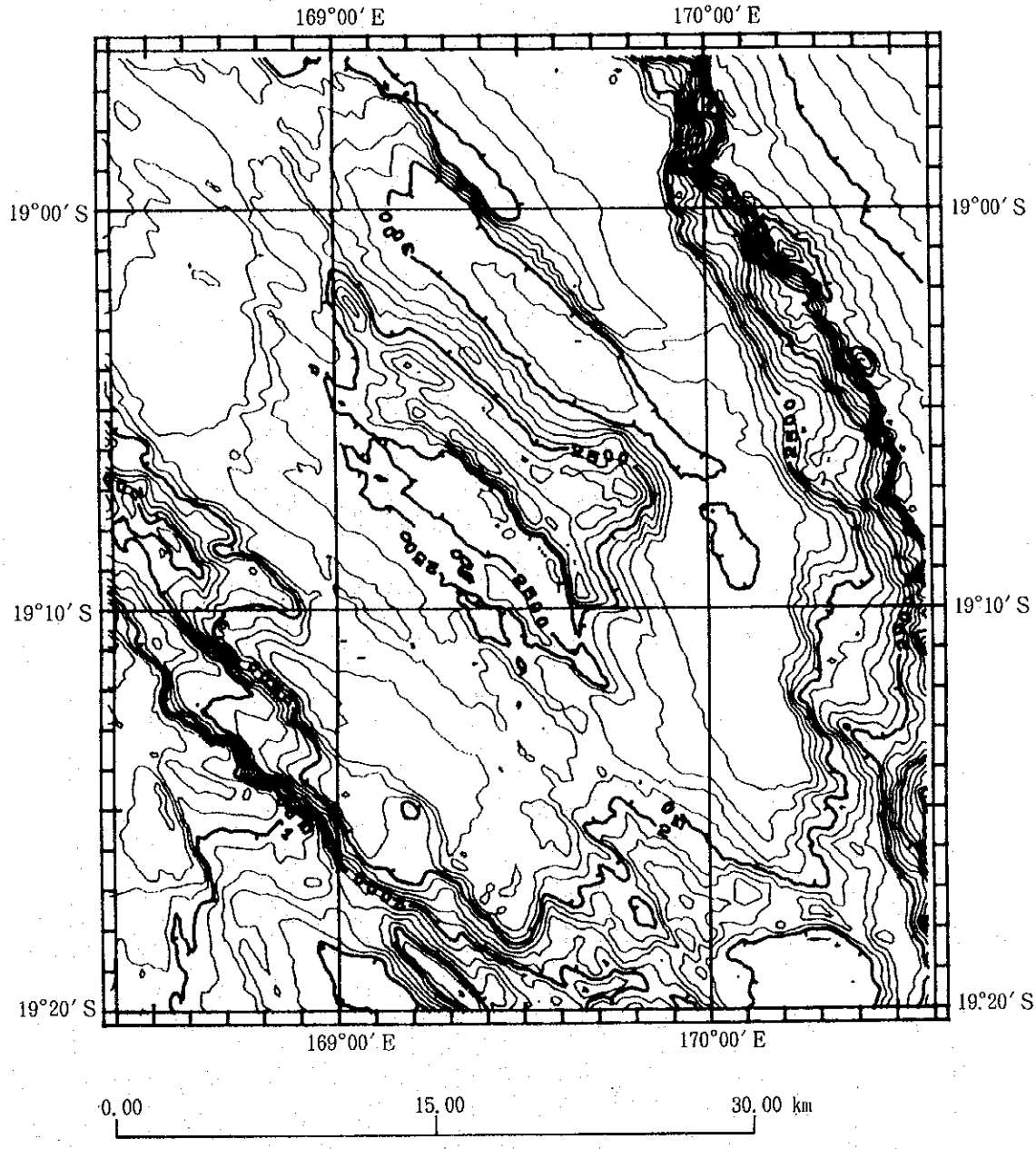

Figure 5-1-3 Bathymetric Map (Erromango Basin)

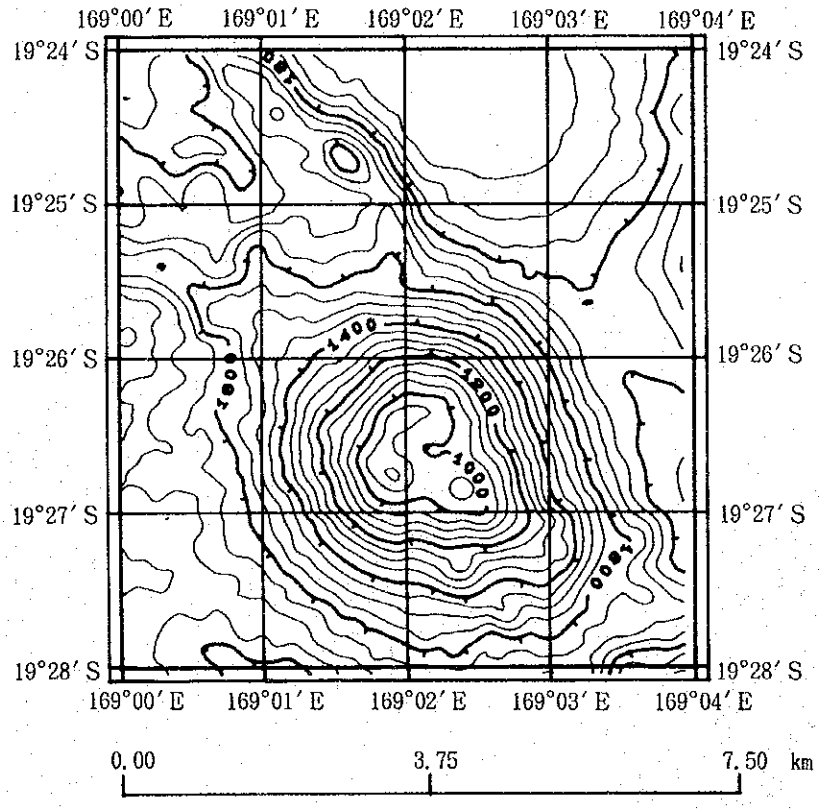

Figure 5-1-4 Bathymetric Map (94S02 Seamount)

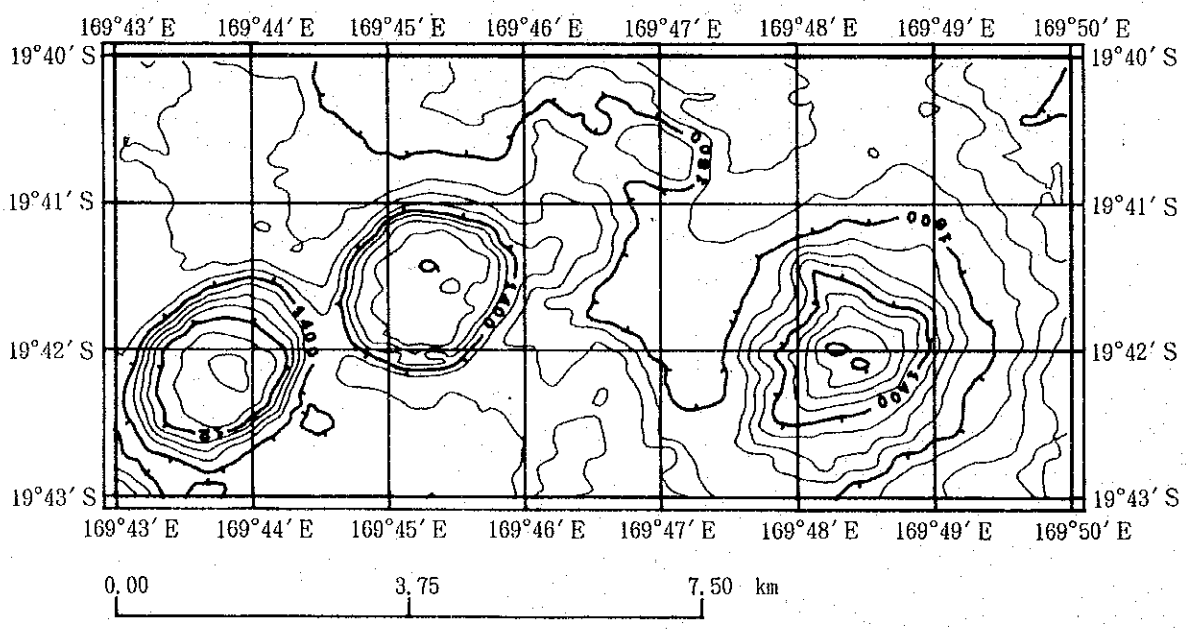

Figure 5-1-5 Bathymetric Map (94S03 Seamount group)

of about 1,200m. They assume relative heights of 300 ~ 400m. The regualrity of seamount arrangement is not conspicuous.

Figure 5-1-5 shows the bathymetric chart of this seamount group.

In conducting the mineral deposit survey, we selected ore indications identified by the FDC survey and then conducted sampling by FPG, CB and LC. For prominent signs of mineralization identified by the FDC survey, we conducted the SSS survey to clarify their scope.

Details of each survey are described in the following sections.

5-2 FDC Survey

We conducted FDC observation at five sea areas, selected as the target areas of the ore deposit investigation.

As the result of FDC observation, relatively extensive ore indications were recognized at three areas (94S01 Seamount, the central part of the Erromango Basin and 94S02 Seamount) and anomalies of water temperature were recognized at two areas (94S01 Seamount and the central part of the Erromango Basin) out of three. For the purpose of this report the term "ore indication" is used as transition intervals (discolored areas) observed by FDC (the same shall apply hereinafter). Hydrothermal communities (biocoenoses) and mounds with chimney-shaped pinnacles were recognized on the 94S01 Seamount, at places where water temperature anomalies were identified.

A fact deserving special mention regarding this year's FDC observation is that we conducted observations at places with a high potential of outcropping rock masses by utilizing the sound pressure chart obtained by the acoustic survey.

Figure 2-6-1 shows the location of each track line, Annexed Figure 4 shows a route map, Figures 5-2-1 (1) ~ (3) show sea-floor photographs taken by FDC, Figure 5-2-2 (1) and (2) show typical photographs of living things taken by FDC, Appendix Table 2 shows a list of FDC survey results and Appendix Table 3 shows a list of ore indications. Ore indication numbers are mentioned in the text and tables as {individual number of the track line} - {order observed} . A new number is assigned when an ore indication seemingly identical with others is found at a different track line.

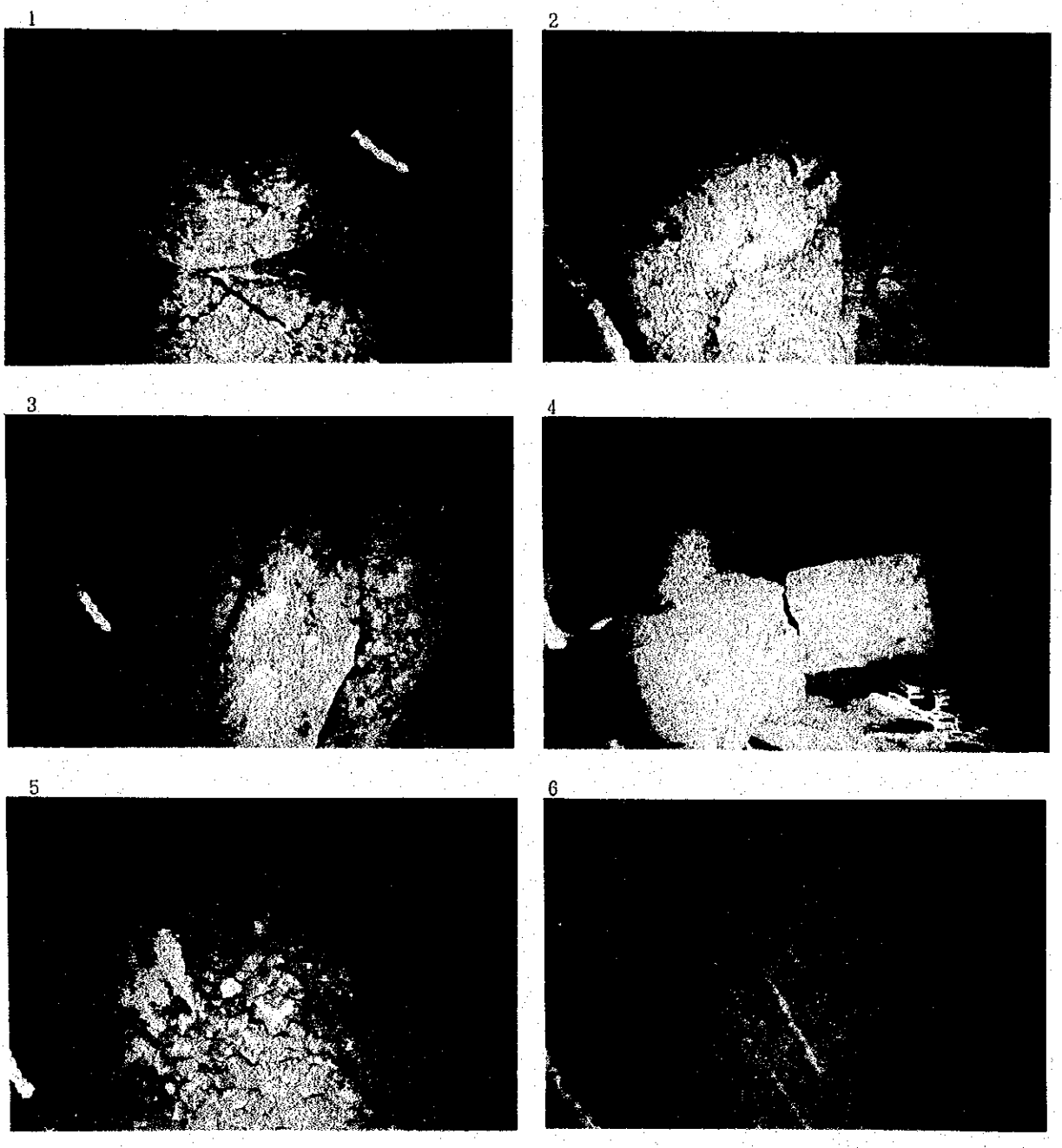

1. Pillow lava — Line94SFDC04 (19°24.12′S, 169°50.83′E, 1,729m)
2. Pillow lava — Line94SFDC06 (19°41.78′S, 169°46.52′E, 1,588m)
3. Sheet lava — Line94SFDC07 (19°41.81′S, 169°48.17′E, 1,389m)
4. Columar joint — Line94SFDC01 (19°02.48′S, 169°50.37′E, 2,201m)
5. Talus — Line94SFDC08-0 (17°56.97′S, 169°24.91′E, 2,679m)
6. Ripple marks — Line94SFDC14 (18°52.92′S, 169°47.47′E, 2,249m)

Figure 5-2-1 Seafloor Photographs taken by FDC (1)

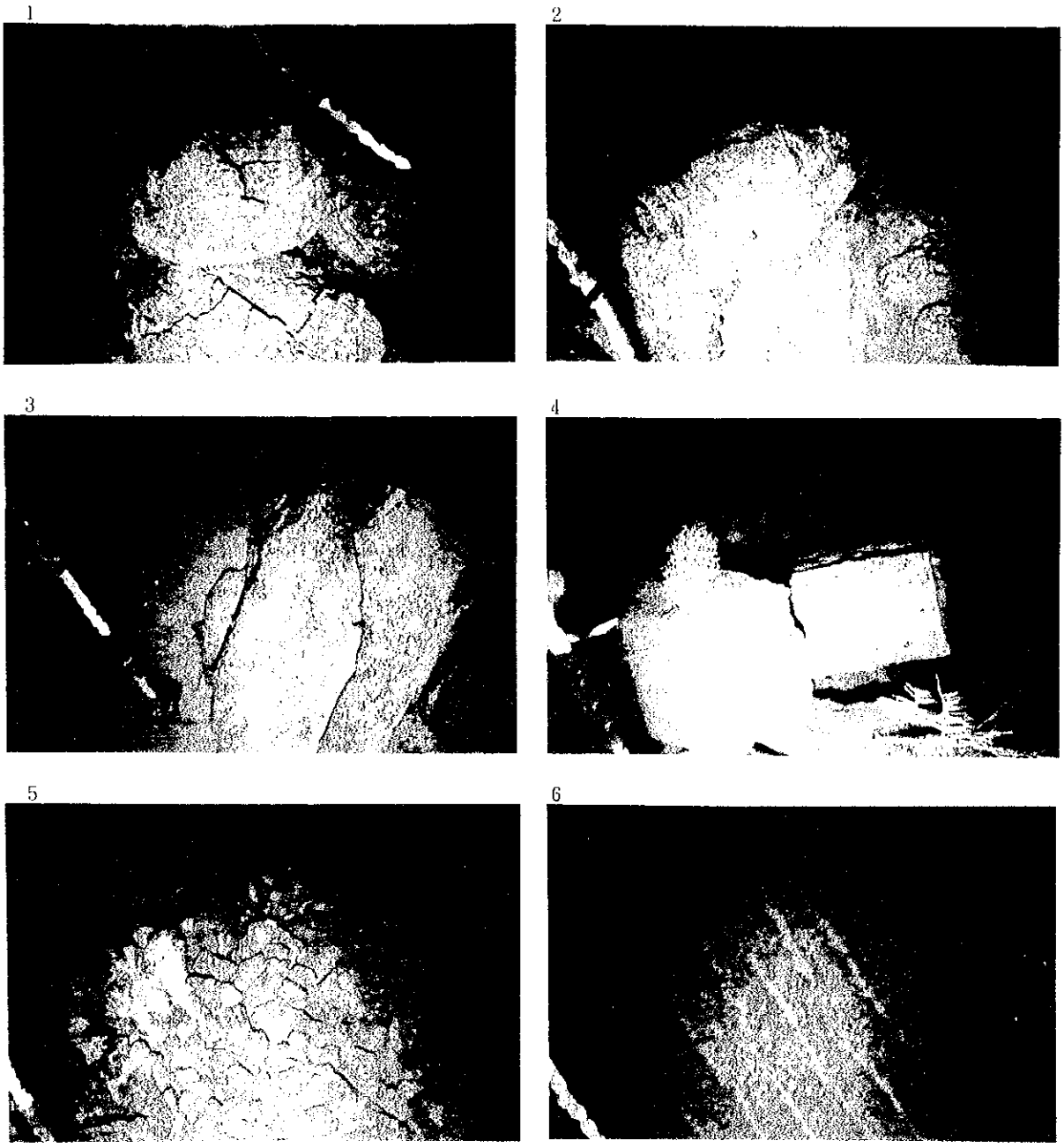

1. Pillow lava — Line94SFDC04 (19°24.12′S, 169°50.83′E, 1,729m)
2. Pillow lava — Line94SFDC06 (19°41.78′S, 169°46.52′E, 1,588m)
3. Sheet lava — Line94SFDC07 (19°41.81′S, 169°48.17′E, 1,389m)
4. Columar joint — Line94SFDC01 (19°02.48′S, 169°50.37′E, 2,201m)
5. Talus — Line94SFDC08-0 (17°56.97′S, 169°24.91′E, 2,679m)
6. Ripple marks — Line94SFDC14 (18°52.92′S, 169°47.47′E, 2,249m)

Figure 5-2-1 Seafloor Photographs taken by FDC (1)

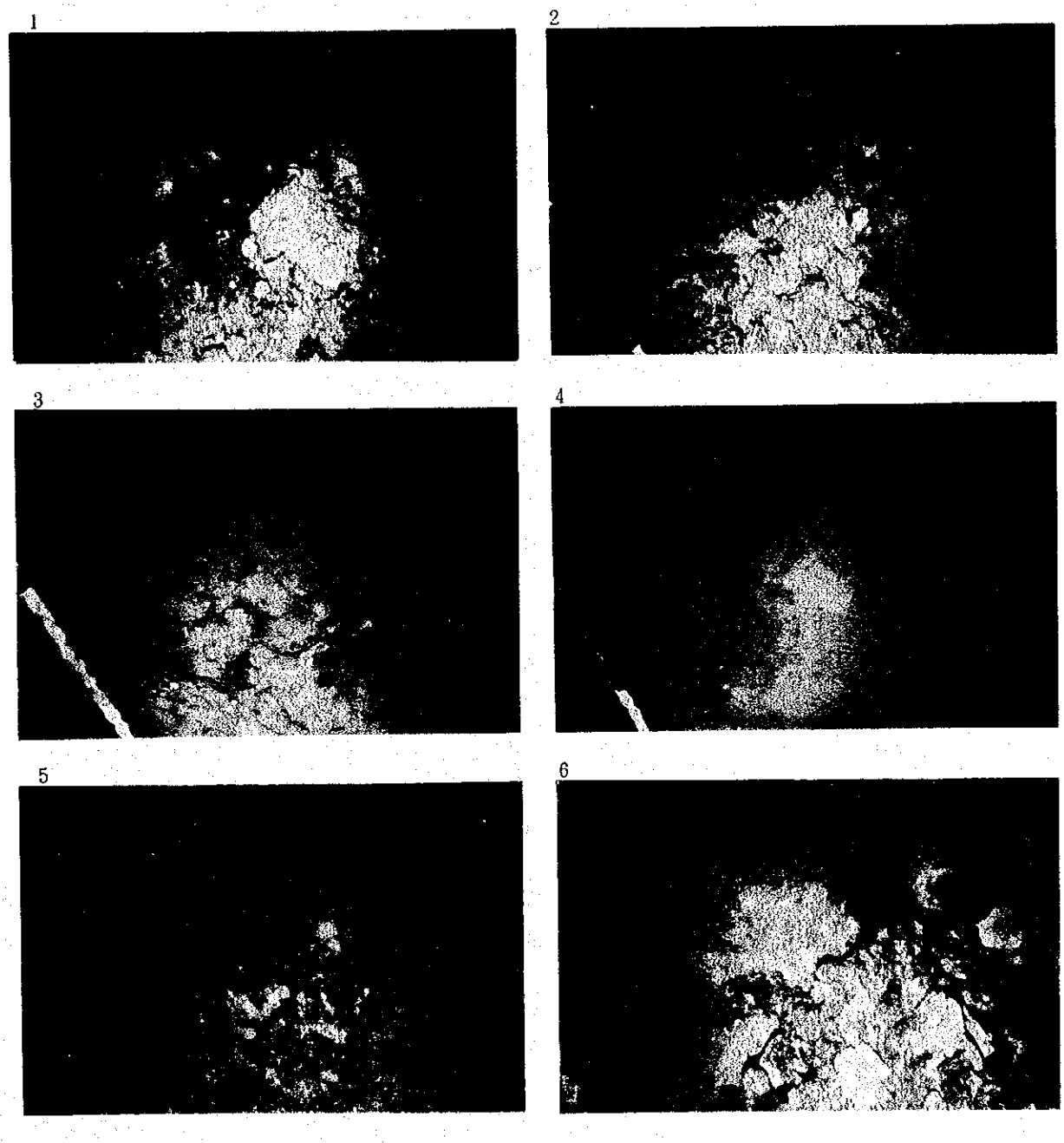

1. Yellowish brown coloured deposit and alterated rock	Line94SFDC01 (19°03.96′S,	169°51.36′E, 2,284m)
2. Yellowish brown and black colored deposit	Line94SFDC01 (19°05.42′S,	169°52.59′E, 2,141m)
3. Yellowish brown colured deposit	Line94SFDC14 (18°53.47′S,	169°48.82′E, 2,291m)
4. Yellowish brown and black colored deposit	Line94SFDC15 (18°59.85′S,	169°54.19′E, 2,450m)
5. Yellowish brown and brown colored deposit	Line94SFDC05 (19°26.66′S,	169°51.95′E, 976m)
6. Brown colured deposit	Line94SFDC05 (19°26.46′S,	169°52.03′E, 937m)

Figure 5-2-1 Seafloor Photographs taken by FDC (2)

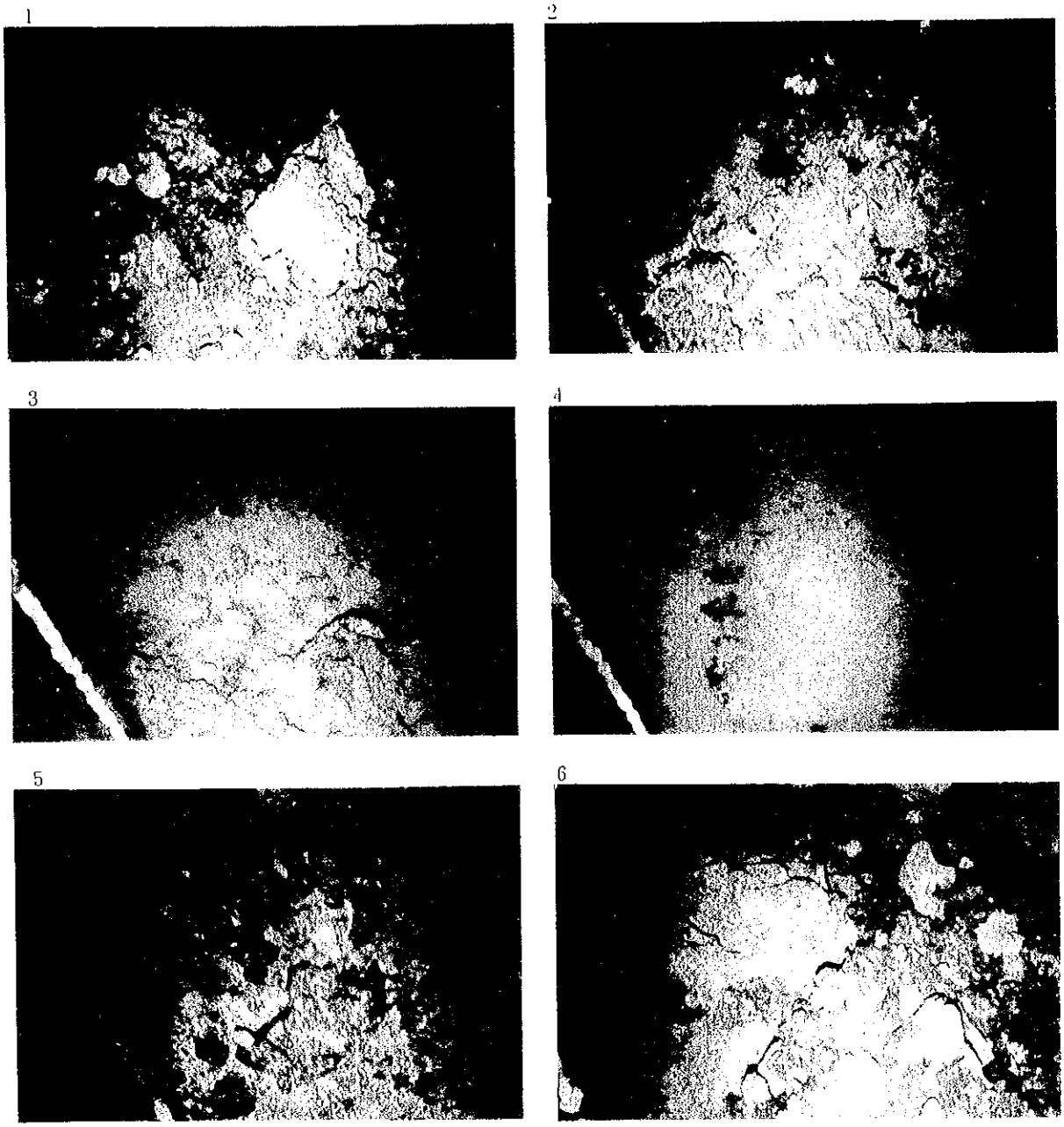

1. Yellowish brown coloured deposit and alterated rock	Line94SFDC01 (19°03.96′S,	169°51.36′E, 2,284m)
2. Yellowish brown and black colored deposit	Line94SFDC01 (19°05.42′S,	169°52.59′E, 2,141m)
3. Yellowish brown colured deposit	Line94SFDC14 (18°53.47′S,	169°48.82′E, 2,291m)
4. Yellowish brown and black colored deposit	Line94SFDC15 (18°59.85′S,	169°54.19′E, 2,450m)
5. Yellowish brown and brown colored deposit	Line94SFDC05 (19°26.66′S,	169°51.95′E, 976m)
6. Brown colured deposit	Line94SFDC05 (19°26.46′S,	169°52.03′E, 937m)

Figure 5-2-1 Seafloor Photographs taken by FDC (2)

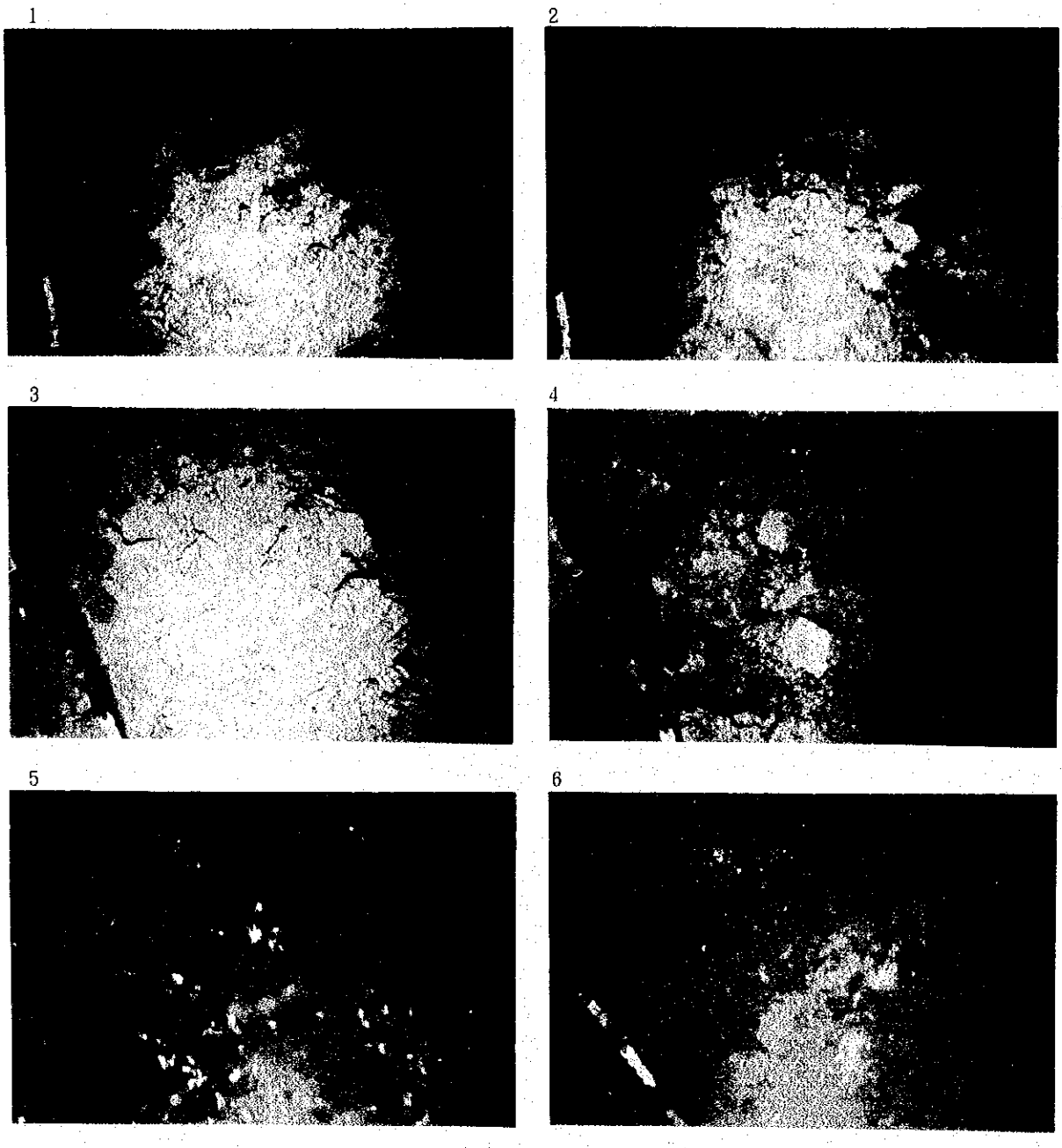

1. Brown colored deposit — Line94SFDC10 (17°34.30′S, 169°05.41′E, 1,198m)
2. Brown colored deposit (vein type) — Line94SFDC11 (17°34.13′S, 169°04.07′E, 1,034m)
3. Brown colored deposit — Line94SFDC12 (17°35.16′S, 169°05.38′E, 1,286m)
4. Brown colored deposit — Line94SFDC12 (17°34.90′S, 169°05.33′E, 1,325m)
5. Brown colored deposit and Munidosis sp — Line94SFDC12 (17°34.39′S, 169°05.40′E, 1,209m)
6. Gastropod & Munidosis sp colony — Line94SFDC12 (17°34.40′S, 169°05.40′E, 1,209m)

Figure 5-2-1 Seafloor Photographs taken by FDC (3)

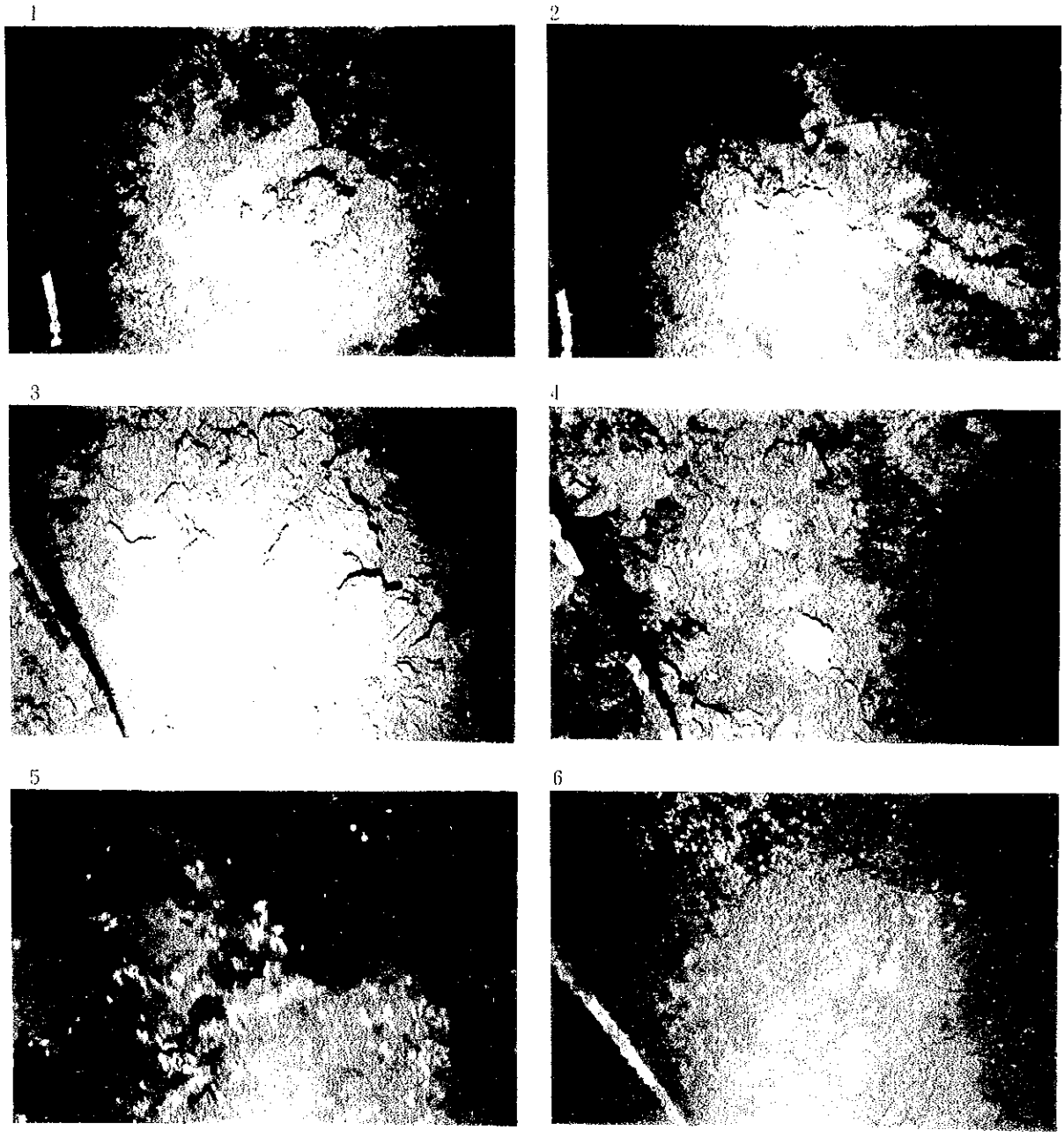

1. Brown colored deposit — Line94SFDC10 (17°34.30′S, 169°05.41′E, 1,198m)
2. Brown colored deposit (vein type) — Line94SFDC11 (17°34.13′S, 169°04.07′E, 1,034m)
3. Brown colored deposit — Line94SFDC12 (17°35.16′S, 169°05.38′E, 1,286m)
4. Brown colored deposit — Line94SFDC12 (17°34.90′S, 169°05.33′E, 1,325m)
5. Brown colored deposit and Munidosis sp — Line94SFDC12 (17°34.39′S, 169°05.40′E, 1,209m)
6. Gastropod & Munidosis sp colony — Line94SFDC12 (17°34.40′S, 169°05.40′E, 1,209m)

Figure 5-2-1 Seafloor Photographs taken by FDC (3)

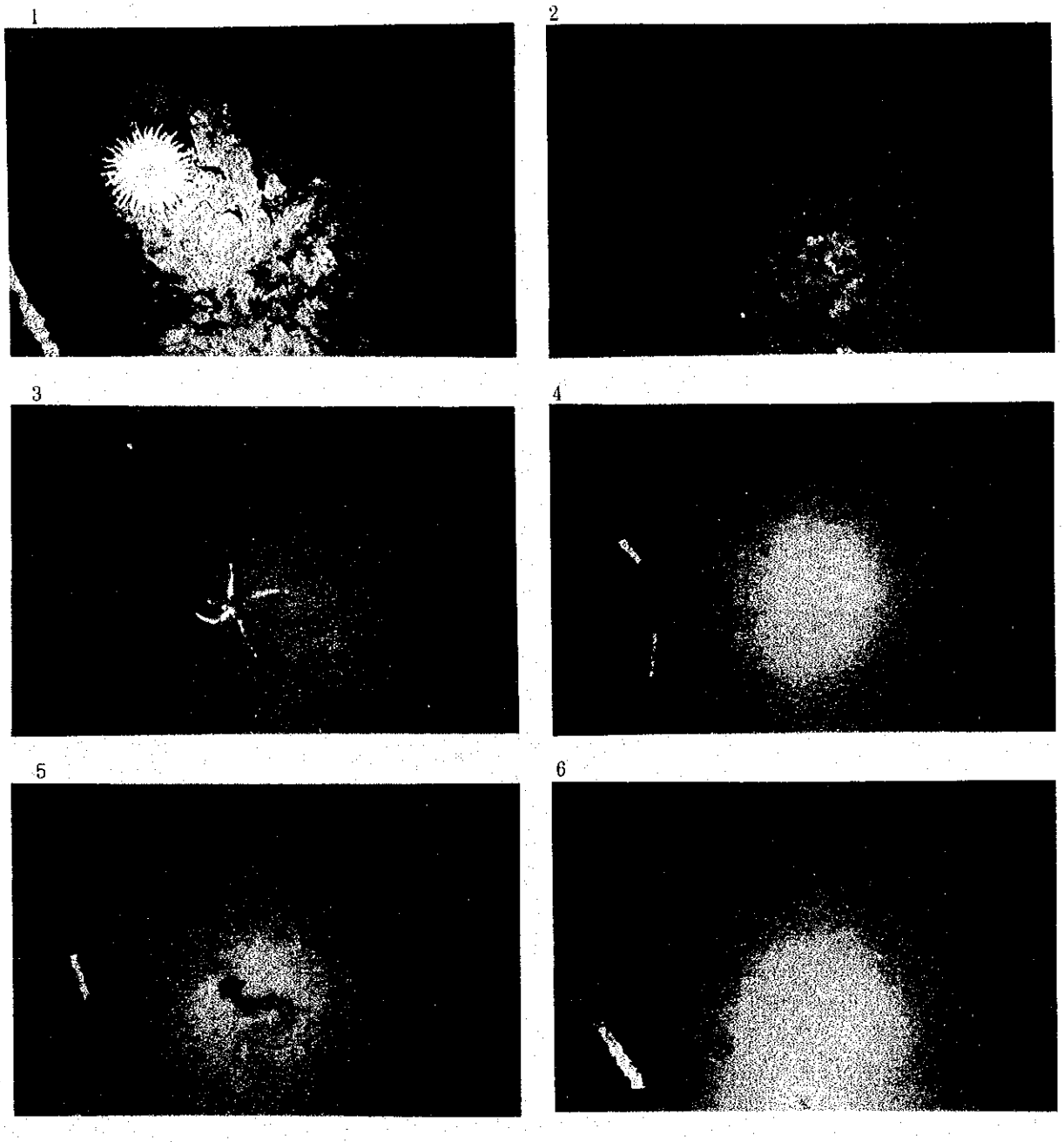

1. Anthozoa — Line94SFDC13 (17°34.57′S, 169°04.22′E, 1,245m)
2. Anthozoa — Line94SFDC02 (19°07.03′S, 169°57.58′E, 2,178m)
3. Asteroidea — Line94SFDC02 (19°05.86′S, 169°56.50′E, 2,623m)
4. Hyglosoma — Line94SFDC17 (19°04.99′S, 169°48.65′E, 2,541m)
5. Lophenteropneusta — Line94SFDC17 (19°04.88′S, 169°48.58′E, 2,564m)
6. Holothurioidea — Line94SFDC08-1 (18°01.89′S, 169°25.08′E, 2,509m)

Figure 5-2-2 Living Things (1)

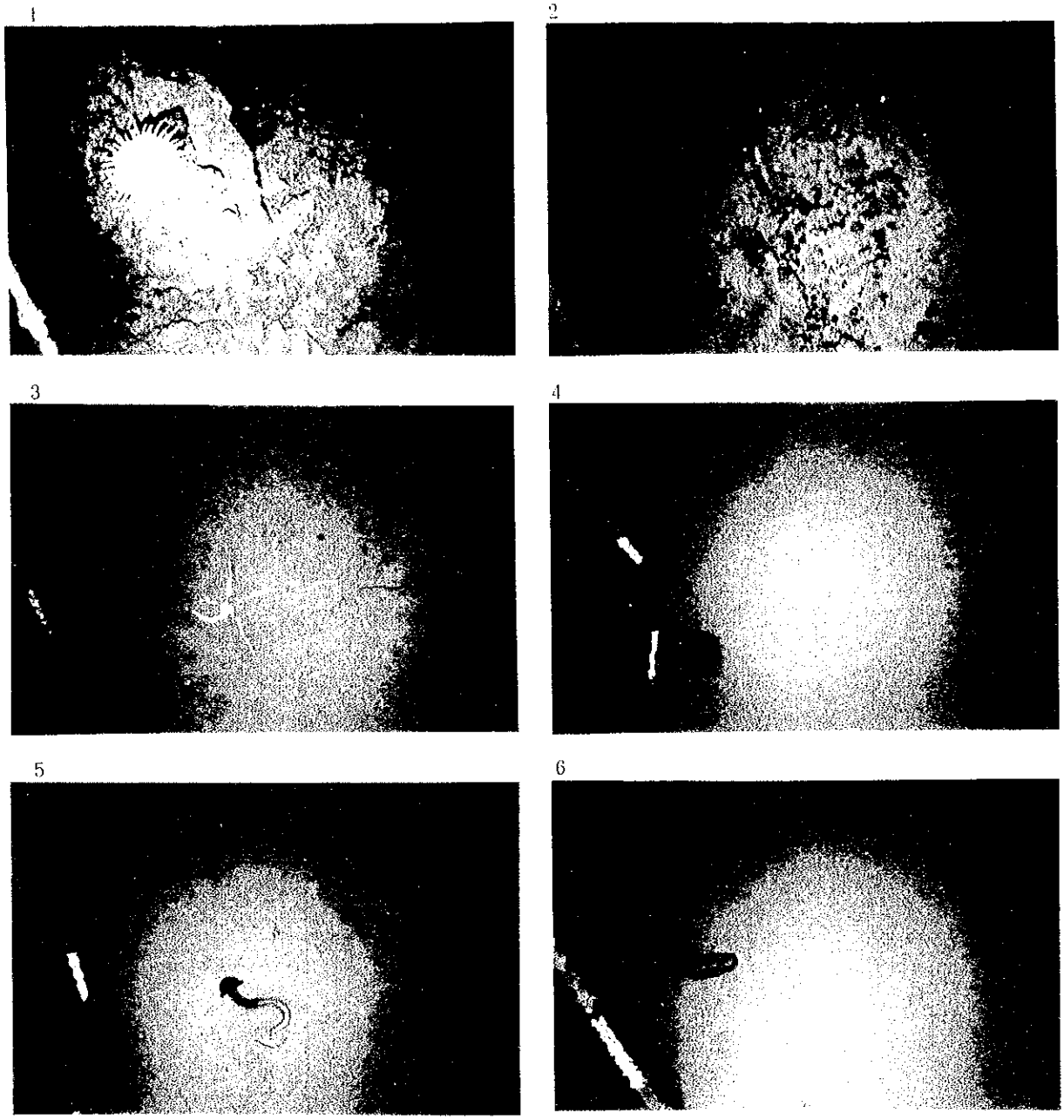

1. Anthozoa — Line94SFDC13 (17°34.57′S, 169°04.22′E, 1,245m)
2. Anthozoa — Line94SFDC02 (19°07.03′S, 169°57.58′E, 2,178m)
3. Asteroidea — Line94SFDC02 (19°05.86′S, 169°56.50′E, 2,623m)
4. Hyglosoma — Line94SFDC17 (19°04.99′S, 169°48.65′E, 2,541m)
5. Lophenteropneusta — Line94SFDC17 (19°04.88′S, 169°48.58′E, 2,564m)
6. Holothurioidea — Line94SFDC08-1 (18°01.89′S, 169°25.08′E, 2,509m)

Figure 5-2-2 Living Things (1)

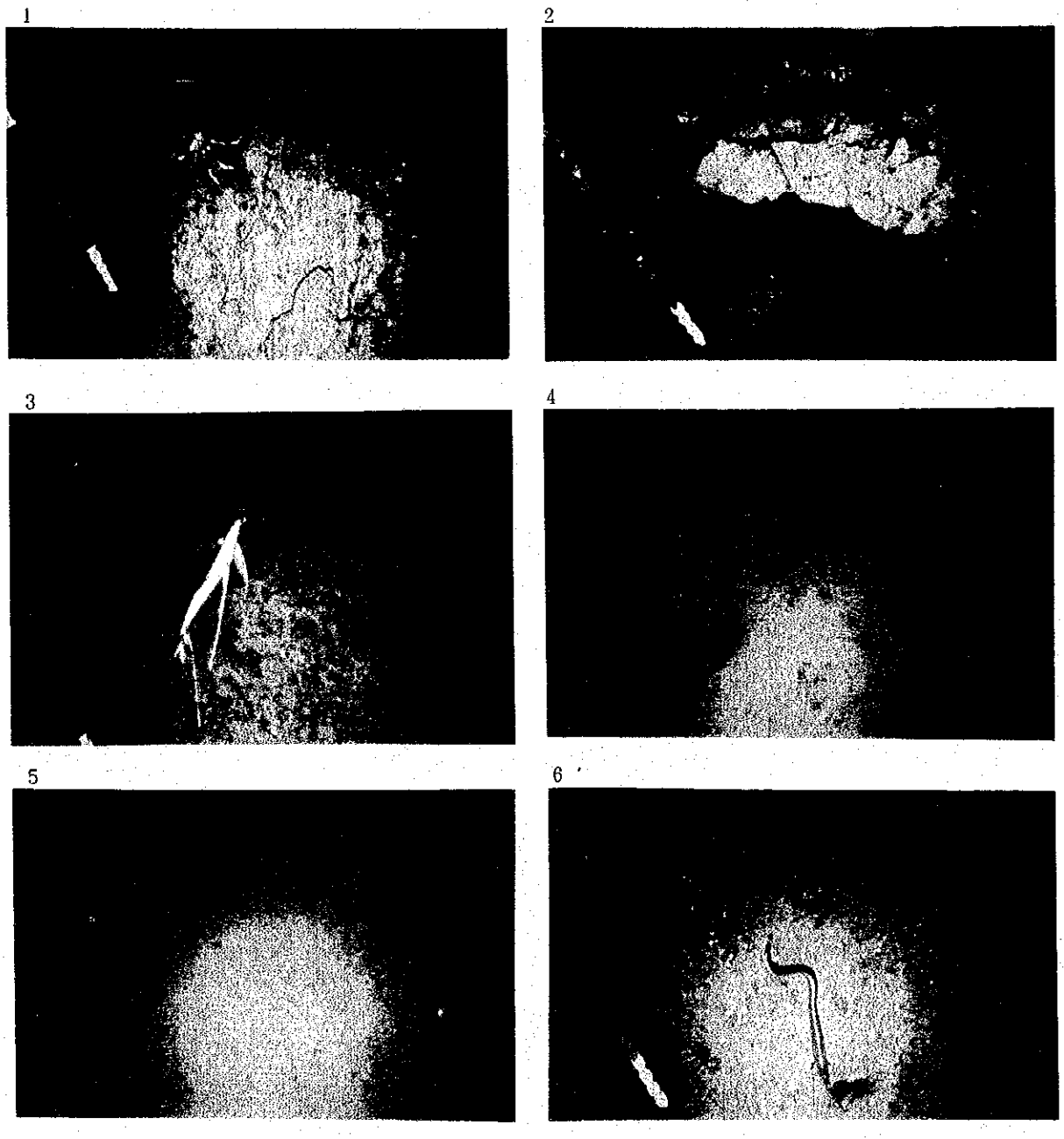

1. Brachyura — Line94SFDC01 (19°06.49′S, 169°54.15′E, 1,979m)
2. Macrura — Line94SFDC12 (17°34.26′S, 169°05.42′E, 1,180m)
3. Benthosaurus — Line94SFDC01 (19°07.14′S, 169°54.98′E, 2,170m)
4. Osteichthyes & Asteroidea — Line94SFDC02 (19°07.01′S, 169°57.68′E, 2,133m)
5. Brotulid fish — Line94SFDC08-1 (18°00.73′S, 169°25.00′E, 2,534m)
6. Halosauridae — Line94SFDC06 (19°41.73′S, 169°45.40′E, 1,220m)

Figure 5-2-2 Living Things (2)

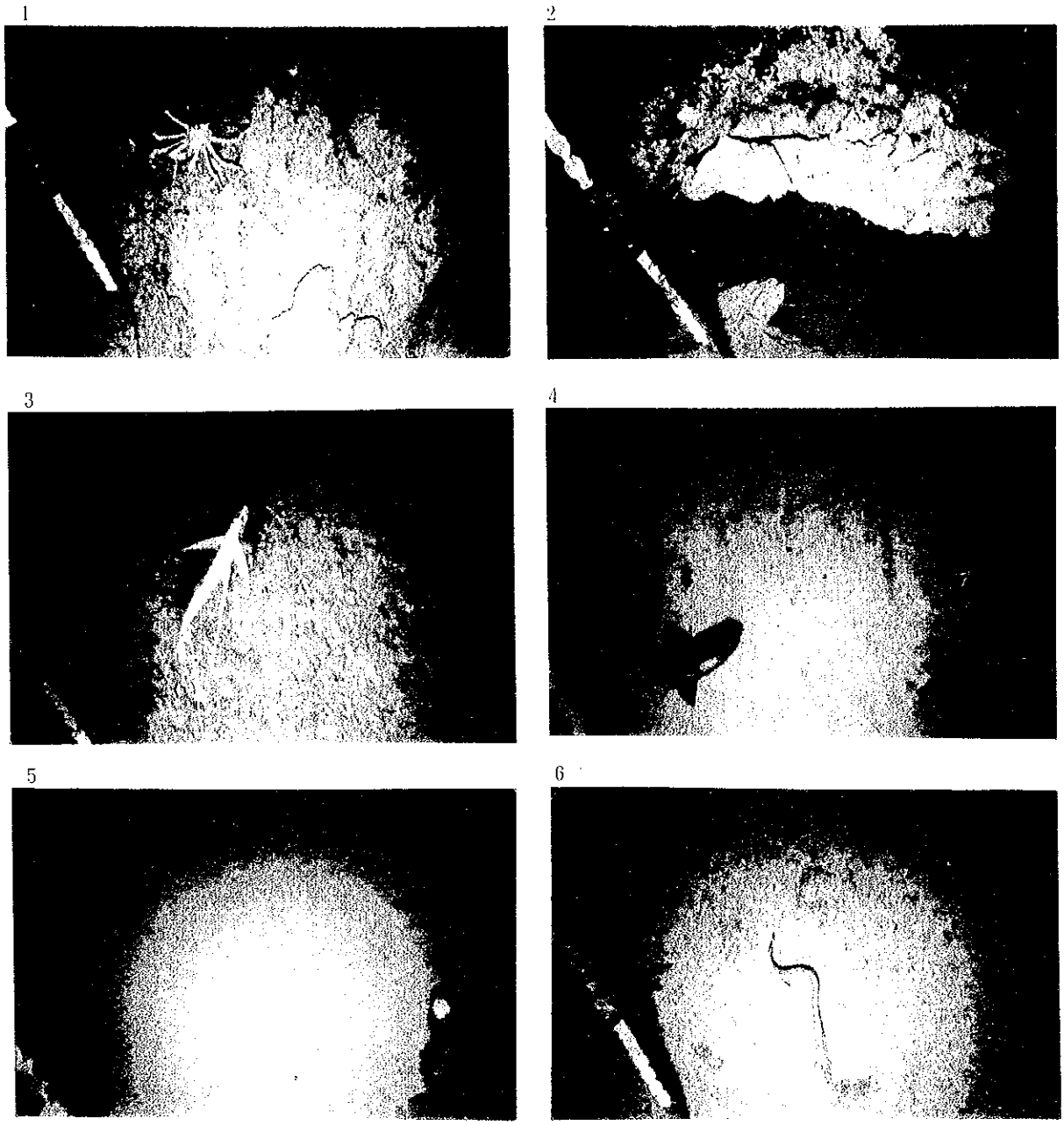

1. Brachyura — Line94SFDC01 (19°06.49′S, 169°54.15′E, 1,979m)
2. Macrura — Line94SFDC12 (17°34.26′S, 169°05.42′E, 1,180m)
3. Benthosaurus — Line94SFDC01 (19°07.14′S, 169°54.98′E, 2,170m)
4. Osteichthyes & Asteroidea — Line94SFDC02 (19°07.01′S, 169°57.68′E, 2,133m)
5. Brotulid fish — Line94SFDC08-1 (18°00.73′S, 169°25.00′E, 2,534m)
6. Halosauridae — Line94SFDC06 (19°41.73′S, 169°45.40′E, 1,220m)

Figure 5-2-2 Living Things (2)

(1) 94S01 Seamount (track lines 94SFDC10 ～ 13)

This seamount is located at the intersection of a tectonic line trending NW-SE and an orthogonal tectonic line. It has an enormous crater in its central part, and it also indicates prominent magnetic anomalies.

From the structural viewpoint, we targeted an area with high sound pressure and a marginal area of crater topography. We then established two track lines running parallel with each other and observed the two targets. Ore indications concomitant with yellowish brown precipitates were recognized at these two track lines (94SFDC10 and 11).

With the objective of identifying the extent theses, we added two more track lines to observe them.

Detailed results of the observation are as follows:

Sediments are poor in every track line but outcrops of rocks are good. Pillow lava, partially slaggy lava and lobate lava are distributed over all track lines. Taluses are distributed over topographically undulating regions and sediments are prominent in flat regions. Isolated signs of mineralization were identified at each of the track lines 94SFDC10 and 94SFDC13 (Ore indication No. 10-1 and 13-1), three ore indications were identified at track line 94SFDC11 (Ore indication Nos. 11-1～3) and four ore indications were identified at track line 94SFDC12 (Ore indication Nos. 12～1-4).

Out of four ore indications found at track line 94SFDC12 three were identified at intersections with the other three track lines. Each of the ore indication is located on the top of a seamount. Each is composed of yellow ～ brown and black precipitates or altered substances, and ore indication recognized at the intersection point of track lines 94SFDC10 and 94SFDC12 (Ore indication Nos.10-1 and 12-2) are concomitant with *Munidopsis, Bythograea thermydron, gastropod* and other hydrothermal communities and ore indication No.12-1 and 12-3 at track line 94SFDC12 are concomitant with chimney-shaped pinnacles. The extent of ore indication is about 930m at ore indication No. 11-1, and about 710m at ore indication No. 10-1. The shortest ore indication is about 70m at ore indication No.13-1 and others are within the ranges of about 200 ～ 500m. Sediments are prominent in the inner area of caldera, and substances appearing to be precipitates are recognized but the continuity is not recognized.

In addition to living things which prefer the hydrothermal environment, such echinoderms as *Crinoidea, Asteroidea, Echinoidea* and *Holothurioidea* such coelenterates as *Anthozoa* and *Osteichthyes, Gorgonian, Macrura, Bythograea thremydron, Porifera, Cnidaria* and other are observed.

(2) Central part of the Vate Trough (track lines 94SFDC080 081 and 09)

As the existence of outcropping rocks and new volcanism in this sea area could be presumed from the existence of high sound pressure zones distributed extensively within the survey area and the presence of magnetic anomalies, we established two track lines: one in a N-S direction (dividing the track line 94SFDC08 into 080 and 081) and another in a NW-SE direction.

As a result, we found that regions with outcropping rocks appear to be basalt are prominent and that these regions correspond to the sound pressure chart, but we could not recognized any ore indications.

Detailed results of the observation are as follows:

Outcrops of rocks were recognized in about 70% of the entire track line 94SFDC08 (the track lines 94SFDC080 and 94SFDC081). Track line 94SFDC09 is very poor in sediments and outcrops of rocks are extremely prominent. Most of the distributed rocks on these two track lines are pillow lava but lobate lava is also found at rare intervals. Taluses are prominent in topographically undulating regions and sediments are prominent at topographically gentle regions. No ore indication were recognized at either track line.

Living things such as echinoderms (*Crinoidea, Asteroidea* and *Holothurioidea*), coelenterates *Anthozoa, Osteichthyes, Gorgonian, Macrura, Bythograea thermydron* and *Porifera* were observed at the track lines 94SFDC080, 081 and 09. Living things which prefer the hydrothermal environment were not recognized.

(3) Central part of the Erromango Basin

1) Central ridge (track lines 94SFDC01 ~ 03)

The observation at track lines 94SFDC01 ~ 03 was made around the ridge located in the central part of the Erromango Basin. Ttrack lines 94SFDC01 and 94SFDC03 were observed in a direction roughly parallel with the central ridge. As for track line 94SFDC02, we observed the northern part of a small crater, where a

ring-shaped, high sound pressure zone was recognized at the eastern marginal part of the central ridge. As a result, a relatively extensive ore indication concomitant with yellowish brown precipitates was recognized at track line 94SFDC01.

Weak ore indication was also recognized at track line 03.

Detailed results of the observation are as follows:

Thickness of sediments are considered to be relatively thin and outcrops of rocks are prominent at track lines 94SFDC01 and 03. Distributed rocks are mainly slaggy lava, sheet lava and subaqueous autobrecciated lava and the distribution of rocks with developed columnar joints is recognized at times. Typical pillow lava is hardly observed. Six places with ore indications were recognized at track line 94SFDC01 (Ore indication Nos. 1-1 ~ 1-6) and one place at track line 94SFDC03 (Ore indication No.3-1). All of the ore indications were composed of yellow ~ brown and black precipitates or altered substances. The extent of ore indications varies greatly. The extent of ore indication No.1-6 (which has the longest continuity) is about 2,060m and Ore indication No.3-1 (which has the shortest continuity) is only a few meters. The ore indications tend to be recognized at regions with a distribution of slaggy lava.

Large part of the track line 94SFDC02 is covered with sediments and, outcrops of subaqueous autobrecciated lava and sheet lava were recognized at times.

No ore indications were recognized at track line 94SFDC02.

Living things such as echinoderms (*Crinoidea, Asteroidea, Echinoidea* and *Holothurioidea*), coelenterates *Anthozoa, Osteichtyes, Gorgonian, Macrura, Bythograea thermydron, Porifera* and *Chidaria* were observed at track lines 94SFDC01 ~ 03. Living things which prefer the hydrothermal environment were not recognized.

2) North ridge (track lines 94SFDC14 and 15)

As we had recognized ore indications on the central ridge, we expected the existence of ore indications or altered zones on the ridge on the north side of the central ridge. Accordingly, we selected a part with specially high sound pressure from the north ridge and established two track lines that parallel the ridge for the purpose of conducting the observation.

Detailed results of the observation are as follows:

Both track lines are extensively covered with sediments and outcrops of rocks

are rare. Sheet lava was distributed at large part of the track line 94SFDC14 and slaggy lava was distributed at large part of the track line 94SFDC15. Taluses are distributed on topographically unduating regions at both track lines.

Black sediments were recognized on normal lntaceous sediments and ripple marks were recognized on the surface of these sediments. Two places with ore indication were recognized at track line 94SFDC14 (Ore indication Nos. 14-1 and 2) and one place with ore indication was recognized at track line 94SFDC15 (Sign No.15-1). Both ore indications were composed of yellow ~ brown and black precipitates or altered substances. Ore indication No.15 -1 was characterized by black precipitate or altered substance and small vents in the sediments. As for the extent of ore indications, Ore indication No.15-1 has continuity of about 620m and Ore indications Nos. 14-1 and 2 have about 40m respectively.

Living things such as echinoderms (*Asteroidea* and *Holothurioidea*), coelenterates *Anthozoa, Osteichthyes, Gorgonian, Macrura, Bythograea thermydron* and *Porifera* were observed at this track line. Living things which prefer the hydrothermal environment were not recognized.

3) South ridge (track lines 94SFDC16 and 94SFDC17)

As we had recognized ore indications at the central and north ridges, we also expected the existence of ore indication at the small-scale ridge on the south side of the central ridge.

So we selected high sound pressure parts from the NBS sound pressure chart and established two track lines for the purpose of conducting the observation.

Detailed results of the observation are as follows:

At track line 94SFDC16, the observation was conducted at the southern part of the Erromango Basin. At track line 94SFDC16, outcrops of rocks were recognized over 80% of the entire track line. Distributed rocks are pillow lava and taluses. Black sediments were recognized all over the track line and ripple marks were observed at rare intervals.

At the track line 94SFDC17, the observation was conducted at the western part of the Erromango Basin. Sediments were prominent throughout the track line and outcrops of rocks were rarely recognized except taluses observed in the neighborhood of cliffs at times. Although a small amount of white sediments covering lutaceous substances were recognized, black sediments were not recognized.

No ore indications were recognized at either track line.

Living things such as echinoderms (*Crinoidea, Asteroidea* and *Holothurioidea*), coelenterates *Anthozoa, Osteichthyes, Gorgonian, Macrura, Bythograea thermydoron* and *Porifera* were observed at the track lines 94SFDC16 and 17. Living things which prefer the hydrothermal environment were not recognized.

(4) 94S02 Seamount (track lines 94SFDC04 and 05)

We selected the seamount which was the largest among the chain of seamounts located on the boundary between the west side of the Futuna Trough and the Erromango Basin with a crater on its top.

We observed around the top of the seamount and a place with high sound pressure and recognized ore indication around the top. With the objective of determining the exten of this ore indication, we added another track line (94SFDC05) and conducted the observation.

Detailed results of the observation are as follows:

Both track lines were poor in sediments and outcrops of rocks were relatively prominent. Pillow lava was mainly distributed at both track lines but distribution of sheet lava and slaggy lava was also recognized. Taluses are distributed on cliffs and undulating places but sediments are prominent on gentle places.

Ore indications were recognized at the top of the seamount where the two track lines intersected (Ore indication Nos. 4-1 and 5-1). The Ore indications were composed of yellow ~ brown and black precipitates or altered substances and the respective range of the ore indications was about 850m.

Living things such as echinoderms (*Crinoidea, Asteroidea* and *Holothurioidea*), coelenterate (*Anthozoa*), and *Osteichthyes, Gorgonian, Macrura* and *Porifera* were observed. Living things which prefer the hydrothermal environment were not recognized.

(5) 94S03 Seamount (track lines 94SFDC06 and 07)

We selected three seamounts distributed on the boundary between the west side of the Futuna Trough and the Erromango Basin as targets. Relatively conspicuous magnetic anomalies are recognized to the south of this seamount group.

We established the track lines by linking the top of the seamounts and places

with high sound pressure.

Detailed results of the observation are as follows:

Sediments are prominently distributed at both track lines and outcrops of rocks are few. White granular sediments were frequently recognized on lutaceous substances and black granular sediments were recognized rare intervals. White sediments are distributed sparsely on the plains but these collected in small holes or small hollows on rocks appeared to be trace fossils. Black sediments cover whole or part of normal muddy substances. These black sediments form ripple marks at times. White sediments were easily stirred up by currents generated by the FDC but black sediments were not. From this and results of sampling, there is a possibility that the white sediments are organic shells and black sediments are volcanic sandy sediments with relatively heavy specific gravity.

Distributed rocks are pillow lava, taluses and slaggy lava.

No ore indications were identified at either track line.

Living things as echinoderms (*Crinoidea, Asteroidea* and *Holothurioidea*), coelenterate *Anthozoa, Osteichthyes, Gorgonian* and *Macrura* were observed. Living things which prefer the hydrothermal environment were not recognized.

5-3 SSS Survey

During the selection of mineral deposit survey targets, especially during the process of selecting FDC track lines, particular attention was paid to ridge-shaped and crater-shaped topography, the areas where submarine reflection sound pressure of MBES suggested the existence of outcropping rocks.

This method was considerably effective, so, with the object of identifying minute topography and distribution of rocks and sediments as well as the extent of ore indications, an SSS survey was conducted at two sea areas among the three sea areas in which ore indications and altered zones had been observed by the FDC survey. The selected two sea areas were the 94S01 Seamount and the Erromango Basin where alteration was prominent.

Figure 5-3-1 shows the SSS track lines and their image maps.

Ore indications observed by FDC coincide with mound-shaped topography and steep taluses near the tops of ridges.

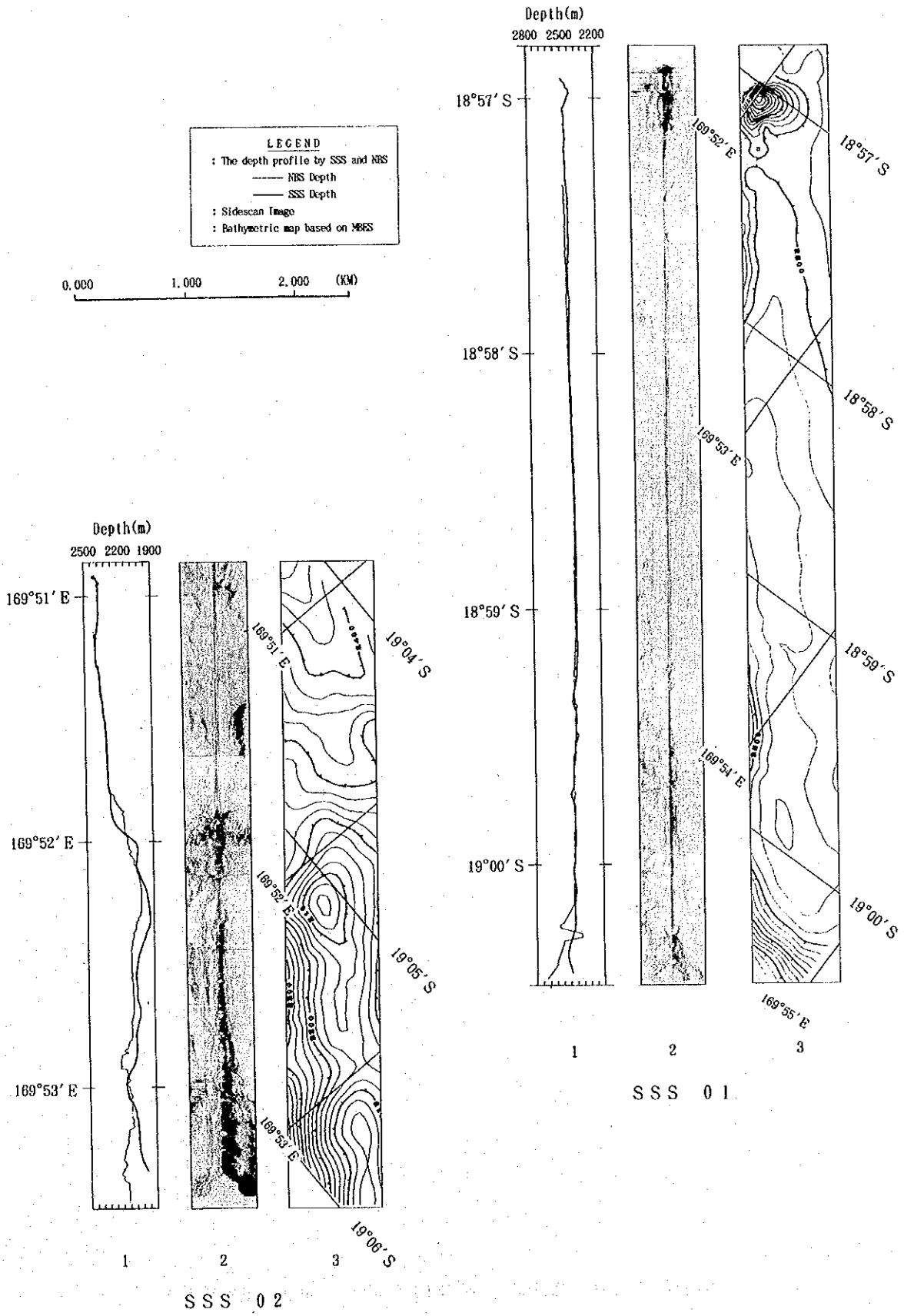

Figure 5-3-1 Results of Side Scan Sonar Survey (1)

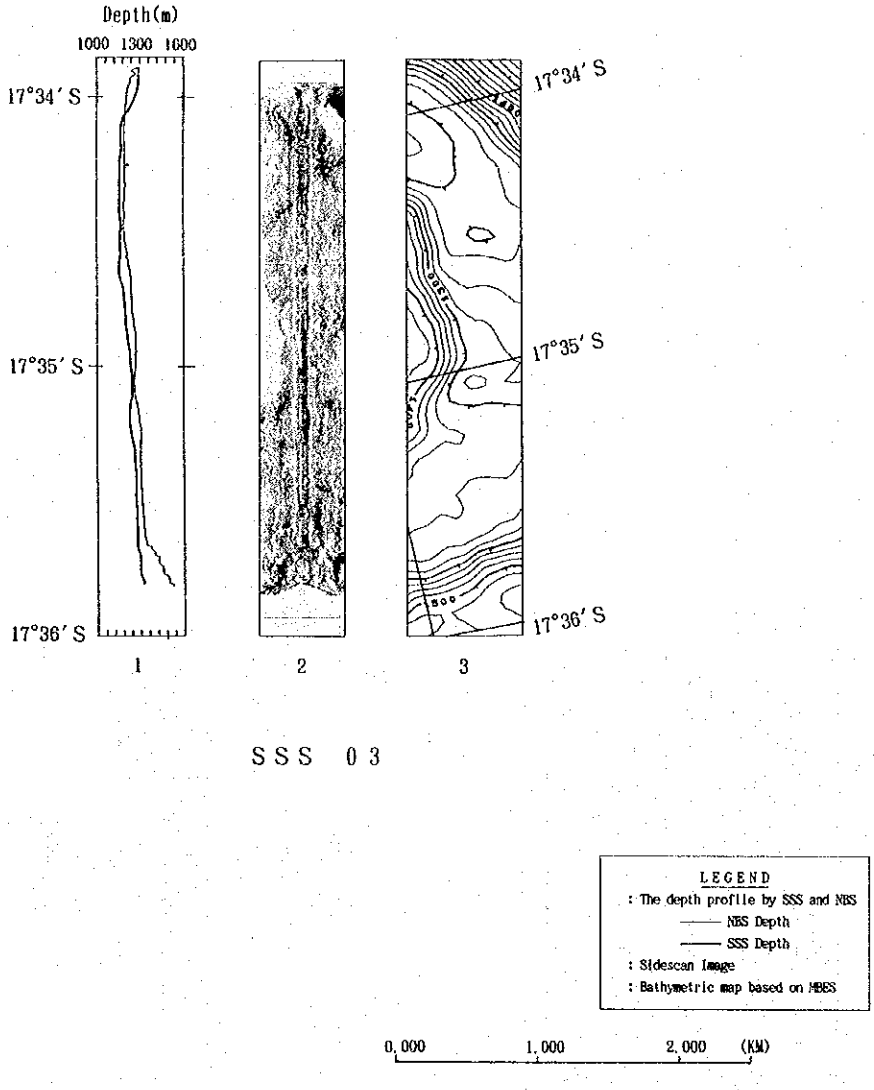

Figure 5-3-1 Results of Side Scan Sonar Survey (2)

(1) 84S01 Seamount

(94SSS03)

The FDC survey was conducted at four track lines (94SFDC10, 11, 12 and 13) covering the caldera on the top of this seamount. And ore indications were observed at every track line, so the SSS survey was conducted along the track line 94SFDC12 that passes the NE ridge and SE ridge on the top of the seamount.

Saddles presumed to be affected by the tectonic line that formed this seamount were seen at the northwestern and southeastern parts of the top embracing the caldera.

There are potentialities that the ore indications observed might be distributed in connection with this tectonic line and that the distributions on the inner side of the northeastern ridge and the southeastern ridge might suggest this. According to the SSS survey a strong reflection was recognized throughout the top except the inside of the caldera, which indicated outcropping rocks. A complex of mound-shaped structures are recognized at the part corresponding to the apparent signs of mineralization observed by FDC. Each mound has a horizontal elongation of less than or about 100m and a relative height of a few meters, which are harmonious with the results of FDC observation. Linear arrangement presumably related to the tectonic line is not clear.

(2) Central part of the Erromango Basin

(94SSS01)

Ore indications of about 100～ 200m were identified on the FDC track line (94SFDC14) that passed by the top of the northern ridge embracing the central graben in the central part of the Erromango Basin. Several transitional intervals covered with sediments at taluses on the southeastern ridge of the main ridge were obtained by FDC images.

Line 94SSS01 was established to clarify the elongation above mensioned zone.

It is said that there is a large possibility of unconsolidated sediments being distributed at parts where sound pressure is low, which are shown as white zone on the SSS images. On the contrary, it is presumed that black zone on the SSS images indicate the distribution of rock masse. Images showing high sound pressure rising linearly along the isobathymetric lines were obtained at a gentle dip part between the low sound pressure part at the lowest part of the top (unconsolidated